LAUNCH WINDOW ANALYSIS FOR ROUND TRIP MARS MISSIONS

Larry A. Manning*
Byron L. Swenson*
Jerry M. Deerwester*

National Aeronautics and Space Administration
Office of Advanced Research Technology
Mission Analysis Division
Moffett Field, California

SUMMARY

Round trip missions to Mars have been investigated to define representative launch windows and associated ΔV requirements. The 1982 inbound and the 1986 outbound Venus swingby missions were selected for analysis and serve to demonstrate the influence of the characteristics of the heliocentric trajectories on the launch window velocity requirements. This report presents results indicating the effects on the launch windows of velocity capability, transfer technique, and of the inclination, eccentricity, and insertion direction of the orbit. The analysis assumed a circular parking orbit at Earth and considers both circular and elliptical parking orbits at Mars. Use of one-, two-, and three-impulse transfers were investigated. The three-impulse transfer employs an intermediate elliptic orbit of 0.9 eccentricity. For all cases, insertion at planet arrival was into an orbit coplanar with the arrival asymptote and any required plane change was performed during the planet departure phase.

The minimum ΔV requirement to transfer from a circular parking orbit to a hyperbolic asymptote occurs when the orbits are coplanar and the maneuver is performed at periapsis of the hyperbola. The study indicates that, using a three-impulse transfer, the ΔV penalty for non-coplanar departures, is no more than 5-10% above the minimum coplanar requirements. Therefore, use in mission analysis of the coplanar ΔV requirements would not result in large errors if three-impulse transfers are acceptable. Use of fewer impulses significantly increases the error. Similar characteristics occur for elliptical parking orbits. However, due to the low coplanar ΔV's, they provide a longer launch window for a given total ΔV capability.

INTRODUCTION

Preliminary analysis of interplanetary missions is generally performed with the assumption that the day-to-day launch window penalties can be closely approximated by the change in the coplanar departure velocity requirements. Since a parking orbit at Earth and/or the objective planet will generally be used, a unique orbit inclination will exist during the launch period of interest. The time dependence of the departure hyperbolic asymptote and the regression of the orbit plane due to planetary oblateness allow essentially coplanar departures for only short time periods. In general, a non-zero angle will exist between the asymptote direction and the orbit plane, and the velocity increment necessary to accomplish the required turning maneuver can be of such magnitude as to render the coplanar assumption invalid.

In this paper, a comparison of three different techniques for performing the turning maneuver from circular orbit during launch windows at both Earth and Mars is made. The techniques consist of optimum one- and two-impulse transfers, and a restricted three-impulse transfer utilizing an intermediate elliptic orbit from which the required plane change is made. In addition, an assessment of using three similar transfers from elliptical parking orbits at Mars is made and the results are compared to the circular orbit results.

To be most meaningful, the departure analysis should be mission oriented. Thus, the orbit escape techniques were applied to two specific Mars stopover missions. These two missions encompass the four trajectory classes of primary interest: i.e., direct inbound and outbound, and Venus swingby inbound and outbound transfers. Therefore, while the quantitative results are not directly applicable to other Mars missions, the conclusions can be generalized to other round trip trajectory modes by utilizing combinations of these transfer trajectories.

The paper is divided into three major sections. The first discusses the orbit transfer techniques which were utilized and provides parametric data in support of the assumptions and approximations made in the analysis. The second section provides the criteria for the mission analysis and defines the characteristics of the 1982 inbound Venus swingby and of the 1986 outbound Venus swingby which were chosen as representative Mars missions. The coupling of the missions with the transfer techniques is contained in the third section, which provides contour maps of constant velocity increments as functions of inclination and staytime in orbit.

METHOD OF ANALYSIS

Orbit Geometry

In considering the launch window problem for a given mission, it is first necessary to establish the relative positions of the orbit plane and the hyperbolic escape asymptote with time. For the analysis of planetary launch windows, it was assumed that the parking orbit at planet arrival was coplanar with the arrival asymptote. The resulting orbit elements are shown in Figure 1. A planet-centered right-hand coordinate system with Z axis at the north pole and X axis at the planet vernal equinox was chosen as indicated. The arrival asymptote or hyperbolic excess velocity vector is defined conventionally as a planet centered vector with right ascension, ρ, and declination, δ. The orbit

*Research Scientist

elements of interest, that is, the inclination, i, and longitude of the ascending node, Ω, are related by

$$\sin(\rho - \Omega) = \frac{\tan \delta}{\tan i}$$

for all $i > \delta$, while the argument of periapsis, ω, is measured from the ascending node.

It can be seen that for each inclination there are two orbit planes coplanar with the arrival asymptote. These two orbits can be distinguished by the relative positions of the spacecraft approach vector at the time of the final midcourse maneuver and the planet centered excess velocity vector. If the spacecraft approaches above the excess velocity vector, it moves initially toward the north pole of the planet and the magnitude of $(\rho - \Omega)$ will be greater than 90°. This orientation shall be referred to as a northern insertion. In the other case, the spacecraft approaches below the excess velocity vector (i.e., toward the south pole) and the magnitude of $(\rho - \Omega)$ is less than 90°. Figure 1 illustrates this configuration which is called a southern insertion.

The situation at some time after arrival is illustrated by Figure 2. The perturbation due to planet oblateness causes the orbit plane to regress about the planet in the manner shown. That is, the inclination of the orbit remains unchanged, the longitude of the ascending node changes by $\Delta\Omega$, and the argument of periapsis changes by $\Delta\omega$ where, to first order in the planet oblateness,[1]

$$\Delta\Omega = -3\pi J_2 \left(\frac{R}{P}\right)^2 (\cos i)\, N$$

$$\Delta\omega = 3\pi J_2 \left(\frac{R}{P}\right)^2 \left(2 - \frac{5}{2}\sin^2 i\right) N$$

and

$$N = \frac{t}{\tau}\left[1 + \frac{3}{2} J_2 \left(\frac{R}{P}\right)^2 \left(1 - \frac{3}{2}\sin^2 i\right)\left(1 - e^2\right)^{1/2}\right]$$

$$P = a(1 - e^2)$$

At that time, the orbit plane makes an angle I_∞ with the departure asymptote.[2]

$$\sin I_\infty = \cos i\,[\sin \delta_d - \tan \delta_r \cos \delta_d \cos(\rho_r - \rho_d - \dot{\Omega}t)]$$
$$\pm[\sin^2 i - \sin^2 \delta_r]^{1/2} \sec \delta_r \cos \delta_d \sin(\rho_r - \rho_d - \dot{\Omega}t)$$

It is this angle which must be compensated for during the departure maneuver.

The orbit geometry at Earth was analyzed in a similar manner except that the initial orbit (corresponding to the orbit at arrival for the planetary case) was chosen in such a manner as to be, through regression, coplanar with the departure asymptote at the nominal departure time; that is, zero plane change was chosen for nominal departure. As with the planetary orbits, two orbital planes exist which satisfy this constraint. These planes are distinguished by the relative position of the spacecraft departure and the departure excess velocity vector at the nominal departure date. If the departure is above the excess vector, then the spacecraft departure is toward the north pole and the magnitude of $(\rho - \Omega)$ is greater than 90°. This departure is called northern injection. The other plane has the spacecraft departing below or south of the excess velocity vector. This case has a $(\rho - \Omega)$ less than 90° and is a southern injection.

Impulsive Analysis

The assumption was made for this analysis that the velocity increments are applied impulsively. The first effect of this assumption is the neglect of gravity losses. Gravity losses, however, are relatively small for these missions and can easily be approximated, or even neglected without significant error.

It can be shown that the orientation between the parking orbit and the escape hyperbola is preserved whether the velocity is added impulsively or through a finite thrusting time. This is indicated by the example in Figure 3 where the velocity increment required to escape to a hyperbolic excess speed of 6.0 km/sec from Mars is shown as a function of the turning angle, that is, the angle between the line of apsides and the departure asymptote. This example is for a departure from an orbit with an eccentricity of 0.9 and 1000 km periapsis altitude. The initial thrust-to-weight ratio for the finite thrusting maneuver was optimized as a function of the true anomaly at the start of thrusting, and varied from about 0.03 near apoapsis, to 0.4 near periapsis.

The primary difference between the results for impulsive thrusting and for finite thrusting is in the position on the parking orbit at which the velocity is added. For finite thrust, the start of thrusting occurs prior to (i.e., leads) the true anomaly for impulsive velocity addition. That is, to obtain the same excess speed and direction as in the impulsive case, the finite thrusting must be approximately centered about the position of the impulsive velocity addition. Typical lead angles are shown in Figure 4. Here, the velocity increment to escape to an excess speed of 6.0 km/sec from Mars is shown as a function of true anomaly around an orbit with an eccentricity of 0.9 and a periapsis altitude of 1000 km. The true anomaly shown for the finite thrust is that at the start of thrusting. It can be seen that for equal velocity increments (and hence equal turning angles) the start of finite thrusting must lead the position for impulsive velocity addition by approximately 5° to 15° in true anomaly for all true anomalies except near apoapsis. Near apoapsis, the associated slow rotation and finite thrust result in a near zero lead angle requirement.

In summary, the assumption of impulsive velocity increments is attractive due to the simplification it permits and appears justified due to the small resultant errors.

Circular Parking Orbit

A comparison of three methods of transfer from a circular parking orbit to a hyperbolic asymptote is provided. These methods are optimal one- and two-impulse direct transfers and a restricted three-impulse transfer using an intermediate elliptical orbit. The techniques are briefly delineated in this section.

One-Impulse Transfers - The single-impulse transfer problem is one of solving for the minimum velocity increment (ΔV) to achieve the desired

hyperbolic asymptote from a specific orbit. The exact solution for minimum ΔV results in an expression which does not permit a closed form solution.[2,3] However, in Reference 3 an approximate solution is developed which provides very good agreement with the exact solution for interplanetary velocity ranges.

Two-Impulse Transfers - The two-impulse transfer technique considered in this study utilizes one impulse at departure from the circular parking orbit and the second impulse at an "infinite" distance from the planet, i.e., at the sphere-of-influence. The solution used was developed in Reference 3 and employs an optimal distribution of velocity change and angle change between the two impulses. Reference 2 considered a transfer with an optimum distribution of velocity between the two impulses and with the second impulse supplying the entire plane change. The parametric results are nearly the same as the optimal transfer employed here.

Figure 5 presents the parametric data for one- and two-impulse transfers. The figure indicates the regions of velocity and plane change requirements where each is superior in terms of minimum total ΔV requirement.

Three-Impulse Technique - The three-impulse mode considered in this study utilizes an in-plane tangential impulse to insert the spacecraft from a circular parking orbit into an intermediate highly-elliptical orbit followed by a plane change at apoapsis to rotate the orbit plane so as to be coplanar with the departure asymptote. The third impulse is then provided tangentially at the appropriate position on the intermediate ellipse so as to place the spacecraft on the required escape hyperbola. The position of the first impulse on the circular parking orbit is varied parametrically and from these results the optimum position is determined by a numerical search. In general, the optimum position is such that the plane change maneuver is minimized without an inordinate penalty for an off-periapsis departure from the intermediate ellipse. A complete analysis of this three-impulse technique has been performed.[4]

A brief study was made of off-apoapsis plane-change maneuvers on the intermediate orbit with the motive of rotating the line of apsides in order to reduce off-periapsis departure penalties. It was found that for highly eccentric orbits very little was to be gained by such maneuvers and that the optimum plane-change position was very near apoapsis. This result is primarily a reflection of the low off-periapsis departure penalties for highly elliptic orbits. The off-apoapsis plane-change option was not retained further in this study.

The effect of the eccentricity of the intermediate ellipse upon the total departure velocity requirements is shown in Figures 6(a) and 6(b) for Earth and Mars, respectively. These data are for a typical hyperbolic excess speed of 6 km/sec and for an orbit altitude of 1000 km. Curves for various values of the angle between the orbit plane and the departure asymptote, I_∞, are shown. It can be seen, especially for large out-of-plane angles, that high eccentricities are very attractive.

Parametric data for the three-impulse departure requirements as a function of hyperbolic excess speed are shown in Figures 7(a) and 7(b) for Earth and Mars, respectively. These data are for an initial circular orbit altitude of 1000 km and an intermediate orbit with an eccentricity of 0.9. Again, various values of the out-of-plane angle, I_∞, are shown. The minimum in departure velocity requirements with hyperbolic excess speed which occurs for the Earth case at rather low values of excess speed as exhibited by the $I_\infty = 30^\circ$ line is due to an increasing off-periapsis departure penalty as excess speed is decreased. That is, for a given I_∞ (non-zero), there is a minimum excess speed below which a periapsis departure is not possible.

Elliptical Parking Orbits

For the elliptical parking orbit, the sum of the arrival and the departure ΔV requirements must be minimized. This approach is necessary since the position of periapsis significantly affects both of the ΔV requirements and the coplanar arrival maneuver will establish that position. In general, both the arrival and the departure will be performed off-periapsis to achieve the minimum total ΔV. For all transfer techniques, the orbit insertion point was varied from $+90^\circ$ to -90° true anomaly on the parking orbit.

As with the circular orbits, three transfer techniques were considered.[5] They are an optimum single impulse and constrained two impulse and three impulse transfers. The techniques are briefly described below.

One-Impulse Technique - In this technique, since both the departure hyperbolic excess vector and the characteristics of the parking orbit at departure are fixed, the non-coplanar, non-tangential departure maneuver true anomaly is iterated to establish the departure point of minimum ΔV requirement for each arrival true anomaly. In general the departure is off-periapsis and has a non-minimum plane change angle.

Two-Impulse Technique - The first impulse is applied at apoapsis to perform the required plane change. The second impulse is applied tangentially near periapsis and provides the required velocity change to achieve the desired excess velocity. Thus, this technique is similar to the last two impulses of the three-impulse transfer from circular orbit.

Three-Impulse Technique - The three-impulse transfer for elliptical orbits is similar to that for circular orbits. The first impulse is applied at periapsis to increase the orbit eccentricity; again, the value of 0.9 was used for the transfer ellipse. The second impulse performs the necessary plane change maneuver at apoapsis and the third impulse applied near periapsis provides the additional velocity increment necessary to achieve the desired hyperbolic trajectory.

MISSION SELECTION CRITERIA

Data to aid in selecting reasonable mission profiles is contained in Ref. 6, which presents mission characteristics for both direct and Venus swingby stopover missions to Mars for each Earth-Mars opposition period from 1980 to the year 2000.

The results of that study indicate that with the exception of the 1984 and 1997 oppositions the swingby

mode is more attractive than the direct mode. Propulsive velocity requirements are consistently lower, in some cases affording reductions of thirty percent. Earth entry speeds are also consistently lower, affording reductions of up to fifty percent. These benefits are realized for mission durations of about 500 days, which represents an increase of about 20 percent over the durations for direct missions (based on thirty-day stopovers). These mission durations were obtained by minimizing the product of propulsive velocity requirements and mission duration. These "nominal" missions from Ref. 6 have mission durations about 25 percent shorter than minimum energy missions at the expense of less than ten percent increase in total propulsive velocity requirements. As will be demonstrated later, such a mission selection procedure contributes to low sensitivity of the mission parameters to launch delays. For the above reasons, and to encompass typical inbound and outbound swingbys, the launch window analyses were conducted for the "nominal" missions from Ref. 6 for both the 1982 inbound swingby and the 1986 outbound swingby.

Since the intent of this paper is to assess the influence of launch delays on mission characteristics, one approach to the selection of the round trip trajectories could have been the specification of a nominal stopover time. This would have necessitated a further specification on the parking orbit characteristics at Mars to ensure that some other criterion be met, e.g., that the nominal departure from Mars be coplanar, or that the plane-change velocity penalty be minimized throughout some arbitrary staytime, etc. The approach taken here is to vary both stopover time and orbit inclination parametrically and to divorce the selection of the outbound leg from the selection of the inbound leg.

Representative Earth departure and Mars arrival conditions must nevertheless be specified. For both mission years considered, the outbound leg chosen is that of the nominal mission employing a 30-day stopover. The Mars departure date was then varied to reflect launch delays. While this may seem restrictive, it is in fact quite reasonable. For outbound swingbys, regardless of mission duration or stopover time, variations of no more than about 10 days arise in either the optimum Earth departure or Mars arrival dates. For inbound swingbys, the variation in Mars arrival date can be on the order of 50 days. However, while the use of the optimum arrival date would reduce the Mars coplanar departure velocity requirements, it does not significantly influence the plane-change requirements for the various stopover times.

This paper is not directly concerned with system characteristics, but recognizing that Mars arrival velocities should not be unconstrained, the outbound legs are selected so that the sums of the Earth departure and Mars arrival velocity increments are equal to the nominal values insofar as possible. When this constant value can no longer be maintained for the longer staytimes, the trajectories are then selected on the basis of minimizing the velocity sum. Note that this procedure is possible by virtue of the manner by which the nominal missions were defined. If the nominal missions had been selected on the basis of minimum energy, then all delays could conceivably cause the velocity requirements to increase. Figures 8(a) and 8(b) illustrate the variation of outbound leg parameters for the 1982 and 1986 missions, respectively.

The technique of maintaining constant velocity is also applied successfully to the definition of the inbound legs in the face of launch delays at Mars as shown in Figures 9(a) and 9(b). In this case, only the Mars departure velocity is considered. Constraints could also be imposed on Earth entry speeds, of course, but as can be seen they remain quite low. To maintain either a constant Mars departure velocity or minimum Mars departure velocity for staytimes in excess of about 60 days, it is necessary for the inbound leg heliocentric transfer angle to exceed 180°. Thus, the inbound leg duration must increase accordingly.

NUMERICAL ANALYSIS

In order to provide an assessment of the performance of one-, two-, and three-impulse transfers, the techniques described for transfer analysis were applied to the two selected missions. This section presents, (1) the results of analysis of the Earth launch window which employs only circular parking orbits, and (2) the results of the analysis of Mars' launch windows employing both circular and elliptical parking orbits.

The format selected for presentation of the launch window data is a contour map, showing lines of constant propulsive velocity requirement on an orbit inclination versus departure date plot. Thus, for a given orbit, the launch window for a given propulsive capability is readily visible. These data are obtained by cross plotting the complete set of transfer data which is computed for fixed inclinations as a function of departure date. The data necessary to prepare the contour maps are included in References 4 and 5.

Earth Launch Window

The launch site considered for these missions was the Kennedy Space Center (KSC). Therefore, the orbit inclinations which can be obtained without a plane change are required to be between the site's latitude ($\approx 28°$) and the range safety constraint (about 50°). The Earth launch window analysis was, therefore, limited to posigrade orbits of 30°, 40°, and 50° inclination.

1982 Inbound Swingby - The results for the 1982 launch are shown in Figures 10(a) and 10(b) for a circular orbit of 300 km altitude and using an intermediate eccentricity of 0.9 for the three-impulse transfers.

Since the variation of the Earth departure hyperbolic excess velocity for this opportunity is from 4 to 5 km/sec, Figure 6 indicates that the two-impulse transfer will have lower ΔV requirements than the one-impulse for plane-change angles (I_∞) over 15°. Figure 10 shows that the two impulse does indeed lower the ΔV requirement at a given departure date. However, for reasonable velocity penalties associated with the plane change (i.e., 10-20 percent of the minimum coplanar departure ΔV) the increase in launch window size (≈ 1 day) is not of sufficient magnitude to make the two-impulse transfer of practical interest.

The use of three-impulse transfers is seen to significantly increase the available launch window. For a ΔV of 4.5 km/sec, the three-impulse window is over 24 days for the southern injection (Fig. 10(a)). For the same ΔV, only a 2-day window is available using one impulse transfers. To achieve a 24-day window with the one-impulse transfer would require a ΔV of 6 to 7 km/sec.

Thus, the increase in launch window flexibility using a three-impulse transfer is such as to make it worth consideration in mission analyses even with the complexity of making three separate maneuvers.

The southern injection orbit rotates relative to the departure vectors such that two coplanar departures occur during the departure period studied. Departures between these points require plane changes and thus ΔV penalties. The three-impulse transfer significantly reduces this plane change ΔV penalty thus opening the region to low ΔV departures. Comparison of Figure 10(a) for the southern injection and Figure 10(b) for the northern injection reveals the effect that the orbit direction can have upon the launch window.

For the northern injection, Figure 10(b), the orbit rotation relative to the departure vector variation is such as to result in only one coplanar departure in a departure period studied. A second coplanar departure occurs at an earlier time. From Figure 8, this earlier departure has a higher Earth departure ΔV requirement. The plane change penalty for this orbit orientation is also higher than for the southern injection. Therefore, the use of a three-impulse transfer for the northern injection orbit results in ΔV requirements about 10% higher than for the southern injection orbit in 1982 for the same window length.

1986 Outbound Swingby - The Earth departure data for the 1986 opportunity is shown in Figure 11(a) for the southern injection orbit, and 11(b) for the northern injection. Conclusions drawn above as to the relative value of one, two, and three-impulse transfers for the 1982 opportunity apply here as well. The effect of orbit orientation is different, however. For this opportunity, it is the northern injection orbit, Figure 11(b), whose rotation, relative to the departure vectors, allows two coplanar departures over the time period studied. Again, use of the three-impulse transfer opens the entire departure region between these coplanar points to low ΔV requirements.

Mars Circular Orbit Launch Window

The minimum inclination which will allow coplanar arrival and departure is defined by the magnitude of the larger of the declinations at arrival and departure. This inclination is 28.7 and 20.8 degrees for the 1982 and 1986 missions, respectively. The maximum inclination is 180° minus the minimum inclination, i.e., a retrograde orbit. The inclinations were, therefore, varied from 30 to 150 degrees for both missions in 10 degree intervals, assuming a circular parking orbit of 1000 km altitude.

Only data for one- and three-impulse transfers are shown in the following sections, since the reduction in ΔV achieved through use of the two-impulse transfer, when a reduction occurred, was small compared to the total ΔV requirement. The three-impulse transfer technique again employs an intermediate orbit with an eccentricity of 0.9 to perform the plane-change maneuver.

Use of the circular parking orbits allows the arrival maneuver to be performed tangentially at periapsis of the arrival hyperbola. The insertion ΔV is, therefore, the same for all staytimes, inclinations and insertion directions. This ΔV is 2.7 and 4.3 km/sec for the 1982 and 1986 Mars arrivals, respectively.

1982 Inbound Swingby - Figures 12(a) through (d) present the contour maps of the ΔV requirements for the 1982 mission. The figures show the data for both southern insertions and northern insertions as previously defined.

Figure 12(a) shows that for a one-impulse escape from a southern insertion orbit, three regions exist having a nearly coplanar departure ΔV requirement (5 km/sec). These are near-polar orbits for staytimes up to 50 days and both low inclination posigrade and high inclination retrograde orbits at 50 days staytime, plus or minus 10 days. In order to provide continuous departure capability up to about 80 days for all available inclinations, a ΔV of 9 km/sec is required. The low ΔV region near 90 degrees inclination occurs since the arrival and departure right ascensions are nearly equal for about 60 days staytime.

Three-impulse transfers from a southern insertion orbit, Figure 12(b), make available low inclinations for short staytimes (5 days) and a low ΔV (5 km/sec) capability. When the ΔV capability is increased to 6 km/sec all inclinations obtainable can be achieved for staytimes up to 70 days. This is a significant improvement over the one-impulse transfer. A similar increase in available staytimes does not occur by increasing the ΔV another 1 km/sec since the coplanar velocity requirement rises rapidly after 60 days staytime (Figure 9(a)).

For this 1982 mission, use of a northern insertion at arrival increases the launch window for a low to moderate ΔV capability. This is shown in Figures 12(c) and (d). The different insertion direction effectively provides an additional 20 days of low ΔV requirement as can be seen by comparing Figures 12(a) and (c). This orbital configuration allows a ΔV of 6 km/sec with a one-impulse transfer to provide staytimes for all inclinations of up to 40 days and for some inclinations of up to 70 days. The three-impulse transfer provides basically the same launch window capability for either orbit insertion since the plane-change penalty is inherently small.

1986 Outbound Swingby - The data for the 1986 Mars launch windows are presented in Figures 13(a) through (d). Between 60 and 70 days staytime a discontinuity occurs in the return leg characteristics. This results from the trajectory selection since the central angle of the transfer conic crosses the 180° ridge. Solutions can, of course, be found in this region by utilizing a finer grid of stay times than was done here, or by constraining the central angle.

Figure 13(a) shows the data for a southern insertion with a single-impulse departure. The data does not display the symmetry shown by the 1982 mission since the arrival and departure right ascensions are at least 45° apart for the first 60 days of staytime. After 60 days, the symmetry is stronger. For near coplanar departure ΔV capability (3.0 km/sec) only small strips of the inclination-staytime map are available. A ΔV of 4 km/sec opens up the low inclination region for staytimes up to about 80 days. However, to achieve polar orbits for this mission, ΔV's of about 5 km/sec would be required if only a one impulse transfer were used.

Comparison of these southern insertion data to Figure 13(b) for a three-impulse transfer reveals the effect of reducing the plane-change penalty. With a

three-impulse transfer, a ΔV of about 3.1 km/sec will allow use of any obtainable inclination for the staytime range shown.

The effect of using a northern insertion at arrival for the 1986 mission is shown in Figures 13(c) and (d). For this mission, the additional low ΔV region at short staytimes, mentioned for 1982, is only about 10 days and does not significantly change the areas available for a given ΔV level. A ΔV of 5 km/sec is required for either insertion to provide a reasonably large inclination-staytime spectrum for single-impulse transfers.

The effect of the different insertion upon the three-impulse data (Figure 12(d)) is negligible with a ΔV of about 3.1 km/sec required to open the entire region of inclinations and staytimes studied.

Mars Elliptical Orbit Launch Window

The analysis was performed for parking orbit eccentricities of 0.3, 0.5 and 0.7 for the 1982 and 1986 missions.[5] Data for all three transfer techniques was developed, but only one- and three-impulse transfers for eccentricities of 0.3 and 0.7 are shown. In the case of the three-impulse transfer, the intermediate orbit for the plane-change maneuver has a 0.9 eccentricity. As with the circular parking orbits, the declinations of the arrival and departure vectors define inclination limits between which the possibility of coplanar arrival and departure exist.

In the analysis of elliptical parking orbits two parameters, in addition to those for the circular parking orbit, are of importance. These are the orbit eccentricity and the location of the line of apsides relative to the arrival and departure asymptote. For circular orbits, the arrival ΔV is a function of the interplanetary trajectory leg and orbit altitude only. However, for elliptical orbits, an off-pericenter insertion maneuver at arrival can reduce the off-pericenter requirement at departure and thus lower the sum of the ΔV's at arrival and departure. The value of the optimal off-pericenter angle at arrival is a function of the inclination of the parking orbit and the desired staytime at the planet. In order to assess the launch window requirements, a nominal staytime is selected and the optimum insertion maneuver for that staytime is defined for each inclination. That insertion maneuver is then held fixed for all staytimes to determine the available departure launch window. Reselection of the insertion maneuver would be expected to produce some gains, but based upon the few cases which were investigated, changes which resulted in reduced ΔV's at long staytimes also resulted in increased ΔV's for short staytimes. In order to decrease the volume of data but still present the salient features of elliptical parking orbits, only data for the better insertion direction of each year as established by the circular orbit data is presented (i.e., northern insertion for 1982 and southern insertion for 1986).

1982 Inbound Swingby - Figure 14(a) presents the total ΔV contours (arrival plus departure) for a one-impulse transfer for an elliptical orbit of 0.3 eccentricity as a function of inclination and staytime. If a coplanar periapsis arrival and departure were possible, a minimum ΔV of 6.6 km/sec could be achieved. As can be seen in Figure 14(a), two small regions exist for which the arrival and departure conditions are sufficiently near the absolute optimum that essentially no penalty occurs. A six percent increase (0.4 km/sec) in the total ΔV results in a staytime of at least 20 days for all inclinations. Using the total ΔV representative of minimum launch windows for circular orbits (7.7 km/sec), a staytime of at least 40 days exists. This is to be compared to the 5-day staytime for the one-impulse transfer from circular orbits.

Data for a three-impulse transfer from a 0.3 eccentricity orbit are shown in Figure 14(b). As in the circular orbit case, an increase in launch window length over the one-impulse transfer occurs. However, the increase is relatively less than for the circular orbits. This is due to the close positions of the arrival vector and the departure vector and their relative magnitudes. For this year, the arrival and departure pericenters are located so that both maneuvers can be performed with one impulse near pericenter since the plane-change requirements are small. A ΔV of 7.7 would produce a launch window of about 48 days for any inclination except near equatorial.

Figure 15 presents the contour plot for a one-impulse transfer from a 0.7 eccentricity parking orbit. For this orbit, the minimum possible ΔV requirement is 5.45 km/sec which is nearly achieved in two regions of Figure 15. An increase of five percent in ΔV to 5.7 km/sec allows a window of 50 days for near polar and high inclination posigrade orbits. The particular form of this ΔV contour in the retrograde region is of interest in that it indicates a departure window of up to 50 days, but not for staytimes below 20 to 40 days at various inclinations. If this early depart restriction is of concern, then the retrograde ΔV requirements are higher than those for posigrade orbits. Use of a ΔV of 7.7 km/sec results in a launch window of 75 days.

The use of a three-impulse transfer from this orbit does not significantly change the launch window contour and is, therefore, not shown.

1986 Outbound Swingby - Data for a one-impulse transfer from a 0.3 eccentricity parking orbit is shown in Figure 16(a). A minimum ΔV requirement of 6.0 km/sec exists for the idealized coplanar, pericenter maneuvers; a minimum of 6.1 was actually achieved. A ΔV of 8.3 km/sec must be allowed before a generally available launch window exists for all staytimes. Even then a significant benefit over the one-impulse transfer from circular orbit does not exist. This occurs since the arrival and the departure asymptotes are over 45° different in right ascension. As a result, the one-impulse case requires a serious compromising of the departure maneuver.

Figure 16(b) presents the contour maps for the three-impulse transfer. In this case, as compared to 1982, the plane change and the departure maneuvers having been optimized individually allows a significant increase in the available launch window. The use of a total ΔV representative of minimum launch windows for circular orbits (7.3 km/sec) results in a launch window of over 60 days for almost all inclinations.

The contour map for a one-impulse transfer from a 0.7 eccentricity orbit is shown in Figure 17(a). For this orbit, the minimum ΔV requirement would be 4.85 km/sec. A value this low was not achieved anywhere on the

one-impulse transfer plot. A ΔV of 7.3 km/sec opens the region below 50° and above 120° for staytimes of 100 days. A ΔV of 8.0 km/sec allows use of the entire contour map.

The results of using a three-impulse transfer from the 0.7 eccentricity orbit are shown in Figure 17(b). Here a ΔV of 6.3 km/sec opens essentially the entire map to use, while a ΔV of only 5.3 km/sec would allow any retrograde orbit.

CONCLUDING REMARKS

This paper provides a summary of the variation in launch windows that can be achieved through use of circular and elliptical orbits and different transfer techniques. The data is presented for two opportunities which are representative of future round trip missions. The data can be used to trade-off ΔV requirements with the complexity of multiple-impulse transfers for all inclinations and staytimes of interest.

To provide departure capability on any day for nominal staytimes up to 60 days at Mars and 20 days at Earth can result in ΔV penalties up to 50 percent of the nominal coplanar ΔV (arrival plus departure) if one-impulse transfers are employed from circular orbits. However, three-impulse transfers from circular orbits permits the same launch windows (i.e., 60 days at Mars and 20 days at Earth) for ΔV penalties on the order of 5-10 percent of the total ΔV requirement.

Elliptical parking orbits do not lend themselves to such general conclusions due to the cross coupling of the arrival and departure maneuvers. Increasing eccentricity of elliptical orbits does, of course, reduce the total ΔV requirement for a given launch window. In addition, the use of three impulses to perform the transfer generally requires lower ΔV's than using a single impulse. However, orbit orientation can exist (e.g., 1982, e = 0.7) for which no gain is shown by the three-impulse maneuver.

As pointed out under the mission selection criteria, supportable, but somewhat arbitrary, ground rules were established to define the interplanetary trajectories. Nominal orbit parameters were established based upon these criteria, thus determining the motion of the orbit as a function of staytime. With an orbit established, reselection of the interplanetary trajectory can be employed to vary the departure characteristics and possibly reduce the ΔV requirements for a particular window. Preliminary data in Reference 4 indicates that reselection of the direct legs does reduce ΔV requirements for single-impulse transfers. Little effect was apparent for three-impulse transfers due to their already low ΔV requirements. Reselection of the swingby leg was also ineffective since the swingby requirement severely restricted planet departure characteristics.

REFERENCES

1. Roy, Archie E., The Foundations of Astrodynamics, The Macmillan Company, New York, 1965, page 224.
2. Deerwester, J. M., McLaughlin, J. F., and Wolfe, J. F., "Earth-Departure Plane Change and Launch Window Considerations for Interplanetary Missions," AIAA Journal of Spacecraft and Rockets, February, 1966.
3. Gunther, P., "Asymptotically Optimum Two-Impulse Transfer from Lunar Orbit," AIAA Journal, February, 1966.
4. Manning, L. A., Swenson, B. L., and Deerwester, J. M., NASA TM, Analyses of Launch Windows from Circular Orbits for Representative Mars Missions, to be published.
5. Manning, L. A., and Swenson, B. L., NASA TM, Analysis of Launch Windows from Elliptical Orbits for Representative Mars Missions, to be published.
6. Deerwester, J. M., and Norman, S. M., "Systematic Comparison of Venus Swingby Mode with Standard Mode of Mars Round Trips," Journal of Spacecraft and Rockets, August, 1967.

APPENDIX A

NOTATION

a	semi-major axis, km
ΔV	propulsive velocity increment, km/sec
e	eccentricity
H	altitude, km
I_∞	minimum angle between departure vector and orbit plane, degs
i	inclination, degs
J_2	second harmonic of planetary oblateness
R	planet radius, km
t	time, sec
V_∞	hyperbolic excess velocity, km/sec
x, y, z	components of the planet centered coordinate system
δ	declination, degs
τ	unperturbed orbital period, sec
ρ	right ascension, degs
Ω	longitude of ascending node, deg
$\dot{\Omega}$	orbital regression rate, degs/day
ω	argument of periapsis, deg

Subscripts

c	circular
d	departure data
i	intermediate ellipse for three-impulse transfer
p	periapsis
r	reference data

FIGURE LEGENDS

Figure 1.- Orbit geometry at planet arrival.

Figure 2.- Orbit geometry at planet departure.

Figure 3.- Effect of finite thrusting time on turning angle.

Figure 4.- Effect of finite thrusting time on ignition true anomaly.

Figure 5.- Optimum one-impulse and two-impulse transfers.

Figure 6.- Effect of eccentricity on three-impulse transfers. (a) Earth orbit. (b) Mars orbit.

Figure 7.- Effect of excess speed on three-impulse transfers. (a) Earth orbit. (b) Mars orbit.

Figure 8.- Outbound leg trajectory characteristics. (a) 1982 inbound swingby. (b) 1986 outbound swingby.

Figure 9.- Inbound leg trajectory characteristics. (a) 1982 inbound swingby (Mars arrival date = 244 5210). (b) 1986 outbound swingby (Mars arrival date = 244 6500).

Figure 10.- Earth departure ΔV contours. (a) 1982 inbound swingby; southern injection. (b) 1982 inbound swingby; northern injection.

Figure 11.- Earth departure ΔV contours. (a) 1986 outbound swingby; southern injection. (b) 1986 outbound swingby; northern injection.

Figure 12.- Mars departure ΔV contours. (a) 1982 inbound swingby; southern insertion; circular parking orbit; one impulse. (b) 1982 inbound swingby; southern insertion; circular parking orbit; three impulse. (c) 1982 inbound swingby; northern insertion; circular parking orbit; one impulse. (d) 1982 inbound swingby; northern insertion; circular parking orbit; three impulse.

Figure 13.- Mars departure ΔV contours. (a) 1986 outbound swingby; southern insertion; circular parking orbit; one impulse. (b) 1986 outbound swingby; southern insertion; circular parking orbit; three impulse. (c) 1986 outbound swingby; northern insertion; circular parking orbit; one impulse. (d) 1986 outbound swingby; northern insertion; circular parking orbit; three impulse.

Figure 14.- Mars ΔV contours. (a) 1982 inbound swingby; northern insertion; parking orbit eccentricity = 0.3; one impulse. (b) 1982 inbound swingby; northern insertion; parking orbit eccentricity = 0.3; three impulse.

Figure 15.- Mars ΔV contours; 1982 inbound insertion; northern insertion; parking orbit eccentricity = 0.7; one impulse.

Figure 16.- Mars ΔV contours. (a) 1986 outbound swingby; southern insertion; parking orbit eccentricity = 0.3; one impulse. (b) 1986 outbound swingby; southern insertion; parking orbit eccentricity = 0.3; three impulse.

Figure 17.- Mars ΔV contours. (a) 1986 outbound swingby; southern insertion; parking orbit eccentricity = 0.7; one impulse. (b) 1986 inbound insertion; northern insertion; parking orbit eccentricity = 0.7; three impulse.

Figure 16.- Mars ΔV contours. (a) 1986 outbound swingby; southern insertion; parking orbit eccentricity = 0.3; one impulse. (b) 1986 outbound swingby; southern insertion; parking orbit eccentricity = 0.3; three impulse.

Figure 17.- Mars ΔV contours. (a) 1986 outbound swingby; southern insertion; parking orbit eccentricity = 0.7; one impulse. (b) 1986 inbound insertion; northern insertion; parking orbit eccentricity = 0.7; three impulse.

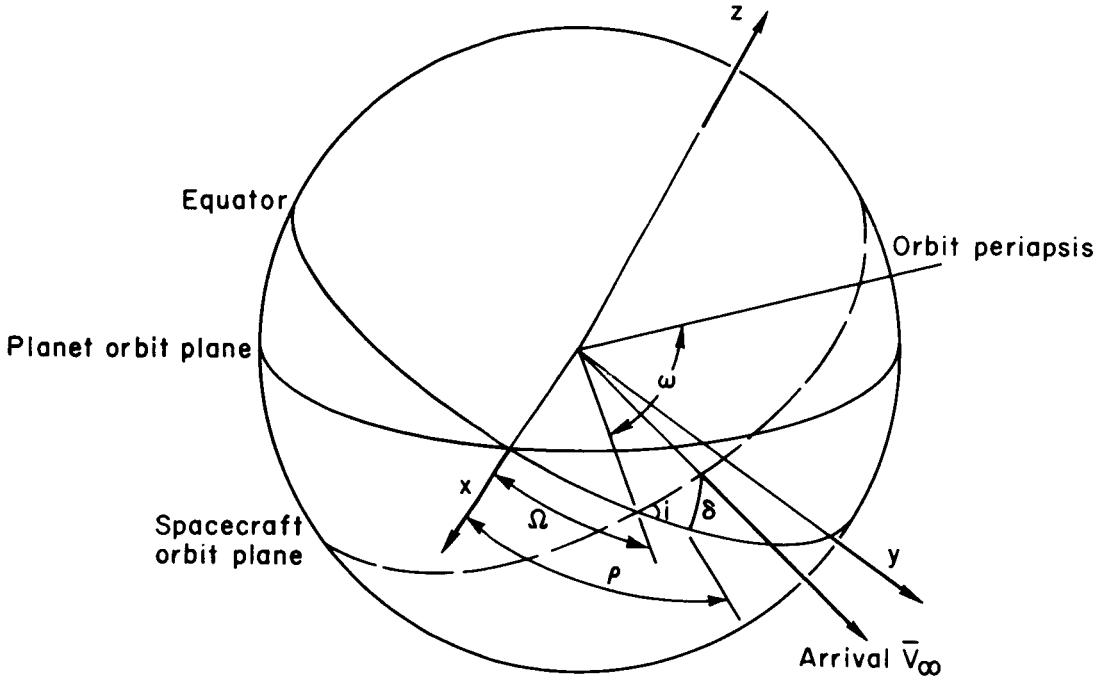
z
Equator
Orbit periapsis
Planet orbit plane
ω
x
Ω
i
δ
Spacecraft
orbit plane
ρ
y
Arrival $\bar{V}_\infty$

Figure 1.

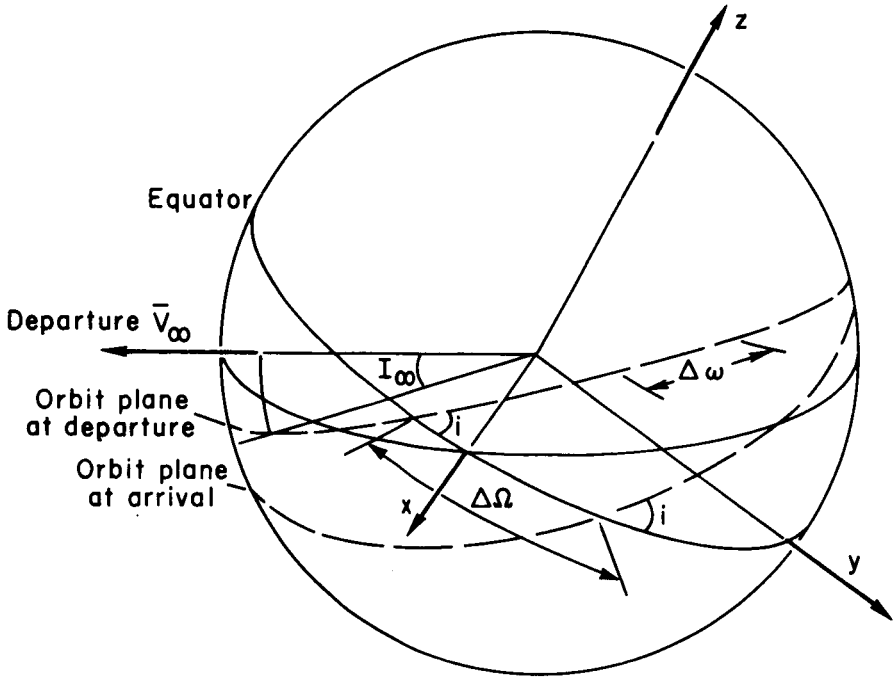
z
Equator
Departure $\bar{V}_\infty$
I_∞
$\Delta\omega$
Orbit plane
at departure
i
Orbit plane
at arrival
x
$\Delta\Omega$
i
y

Figure 2.

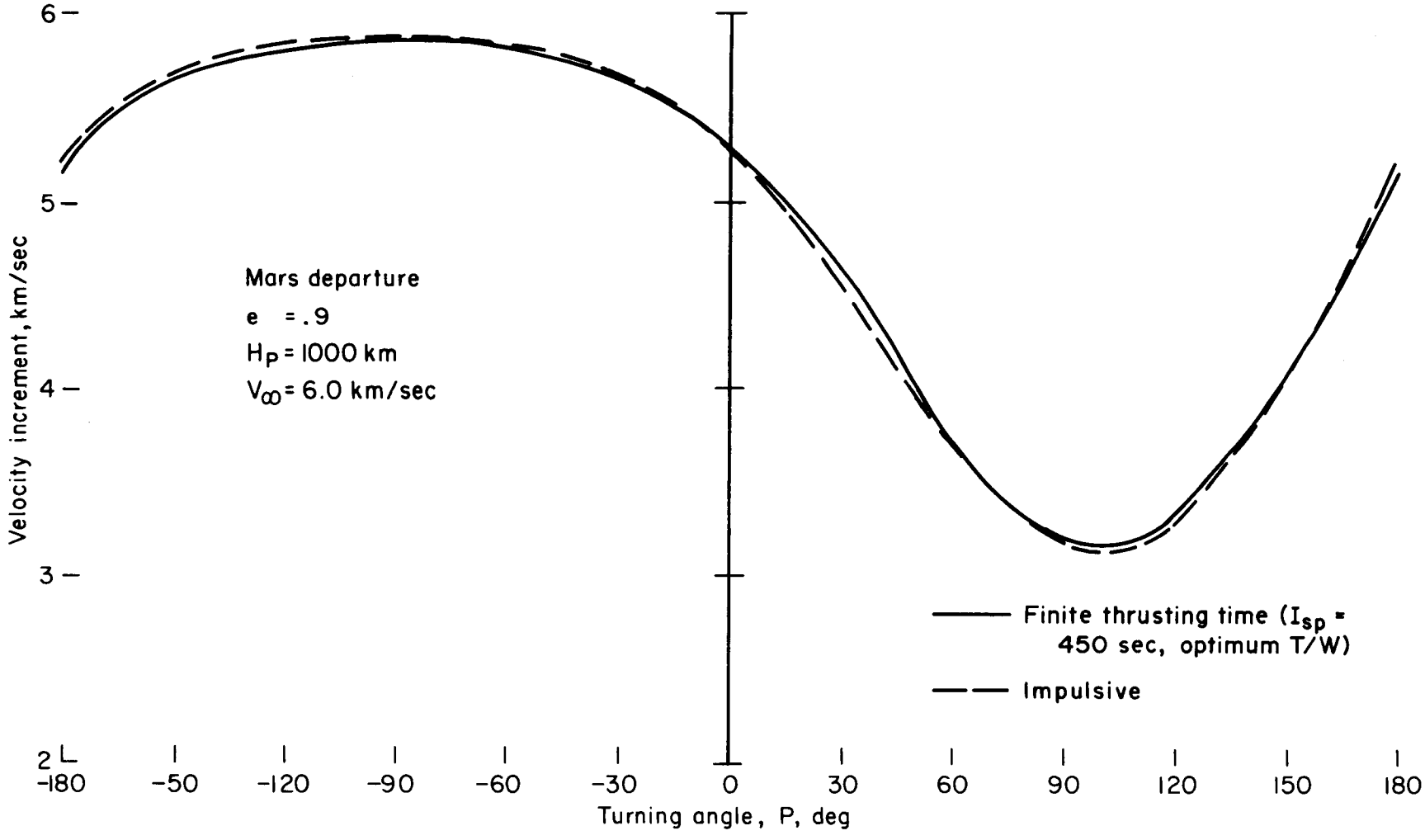

Figure 3.

NATIONAL AERONAUTICS AND SPACE ADMINISTRATION
AMES RESEARCH CENTER, MOFFETT FIELD, CALIFORNIA

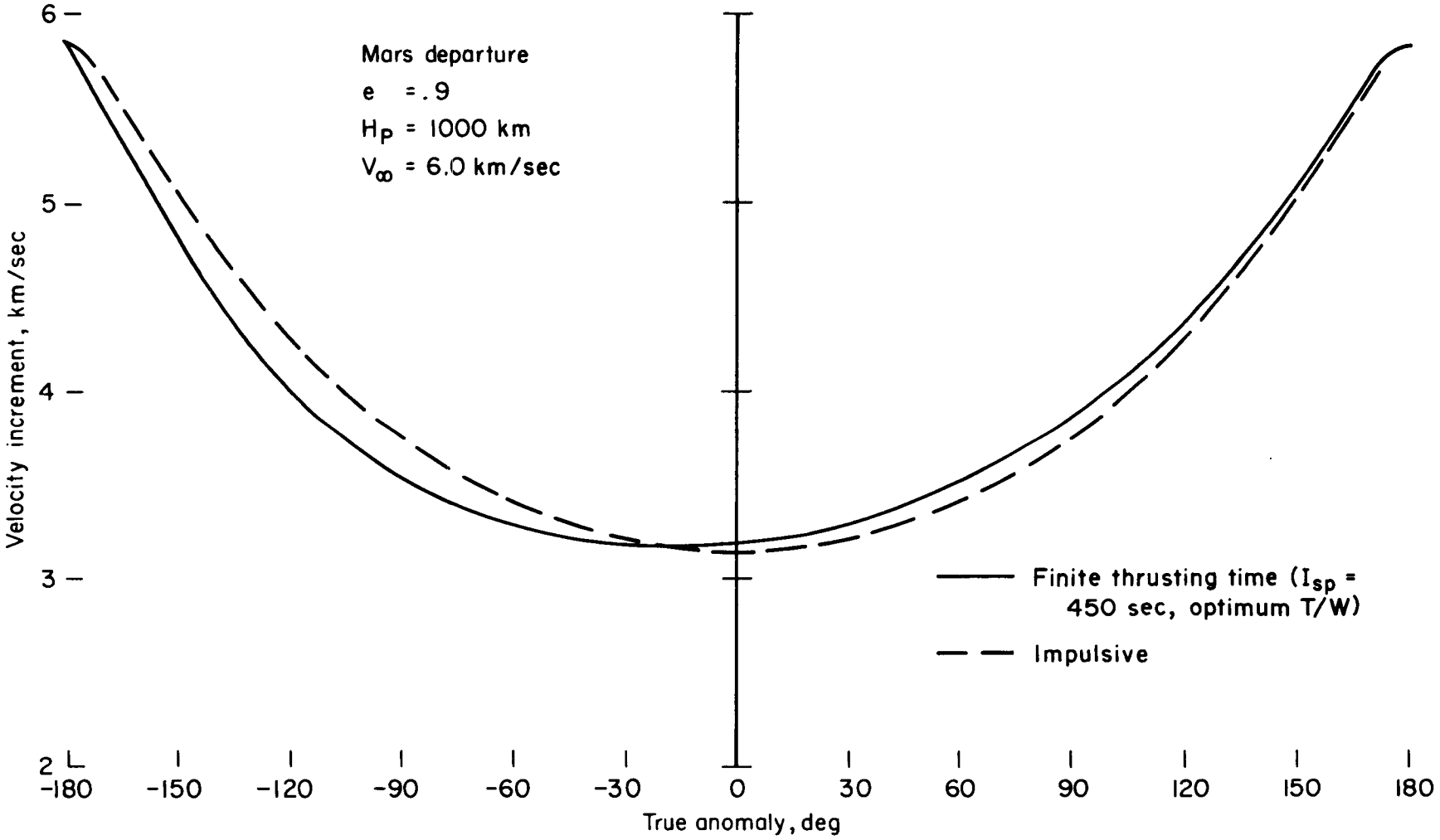

Figure 4.

NATIONAL AERONAUTICS AND SPACE ADMINISTRATION
AMES RESEARCH CENTER, MOFFETT FIELD, CALIFORNIA

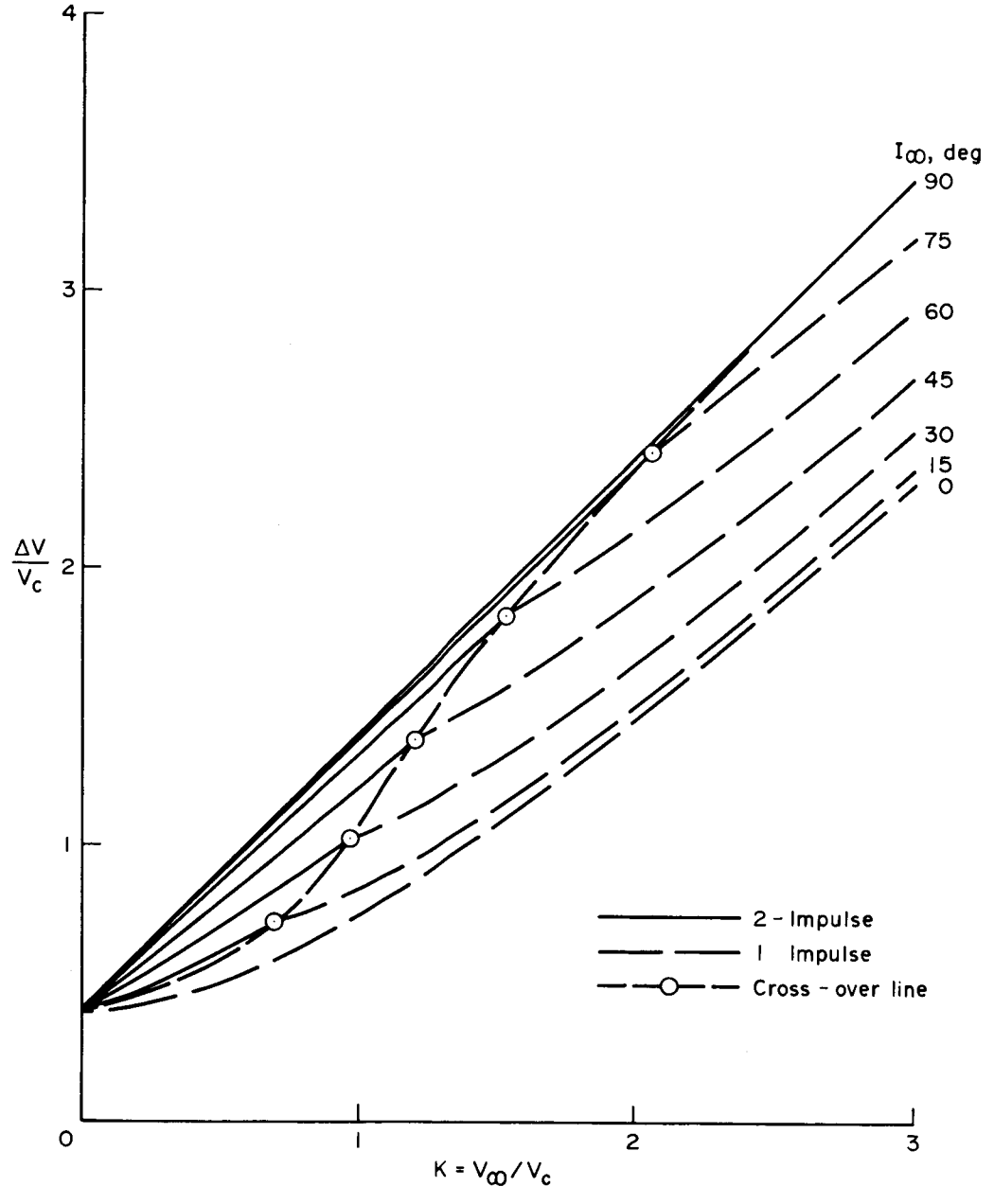
4
3
2
1
0
$\frac{\Delta V}{V_c}$
I_∞, deg
90
75
60
45
30
15
0
2 - Impulse
1 Impulse
Cross - over line
1
2
3
$K = V_\infty / V_c$

Figure 5.

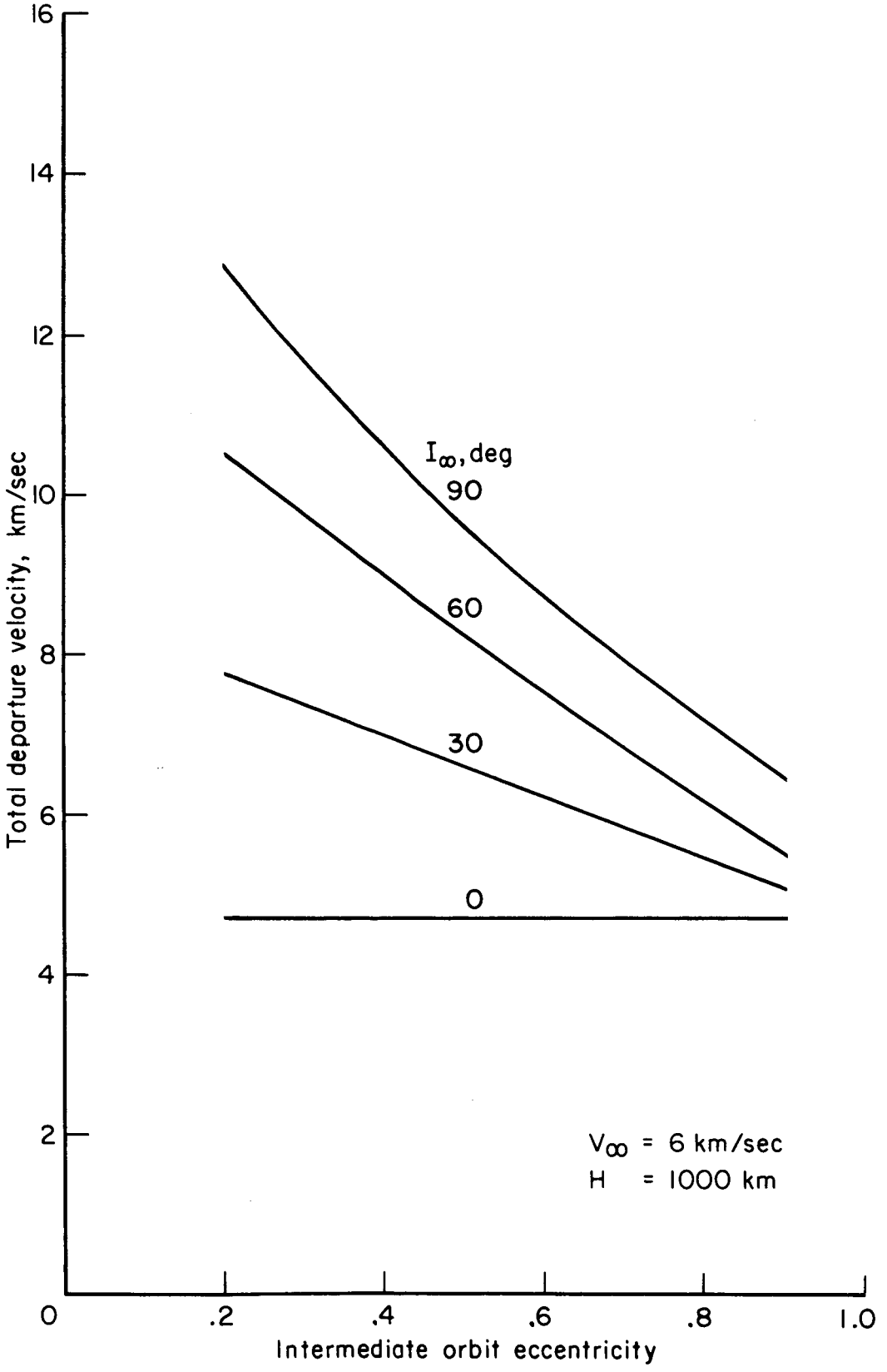

Figure 6(a).

NATIONAL AERONAUTICS AND SPACE ADMINISTRATION
AMES RESEARCH CENTER, MOFFETT FIELD, CALIFORNIA

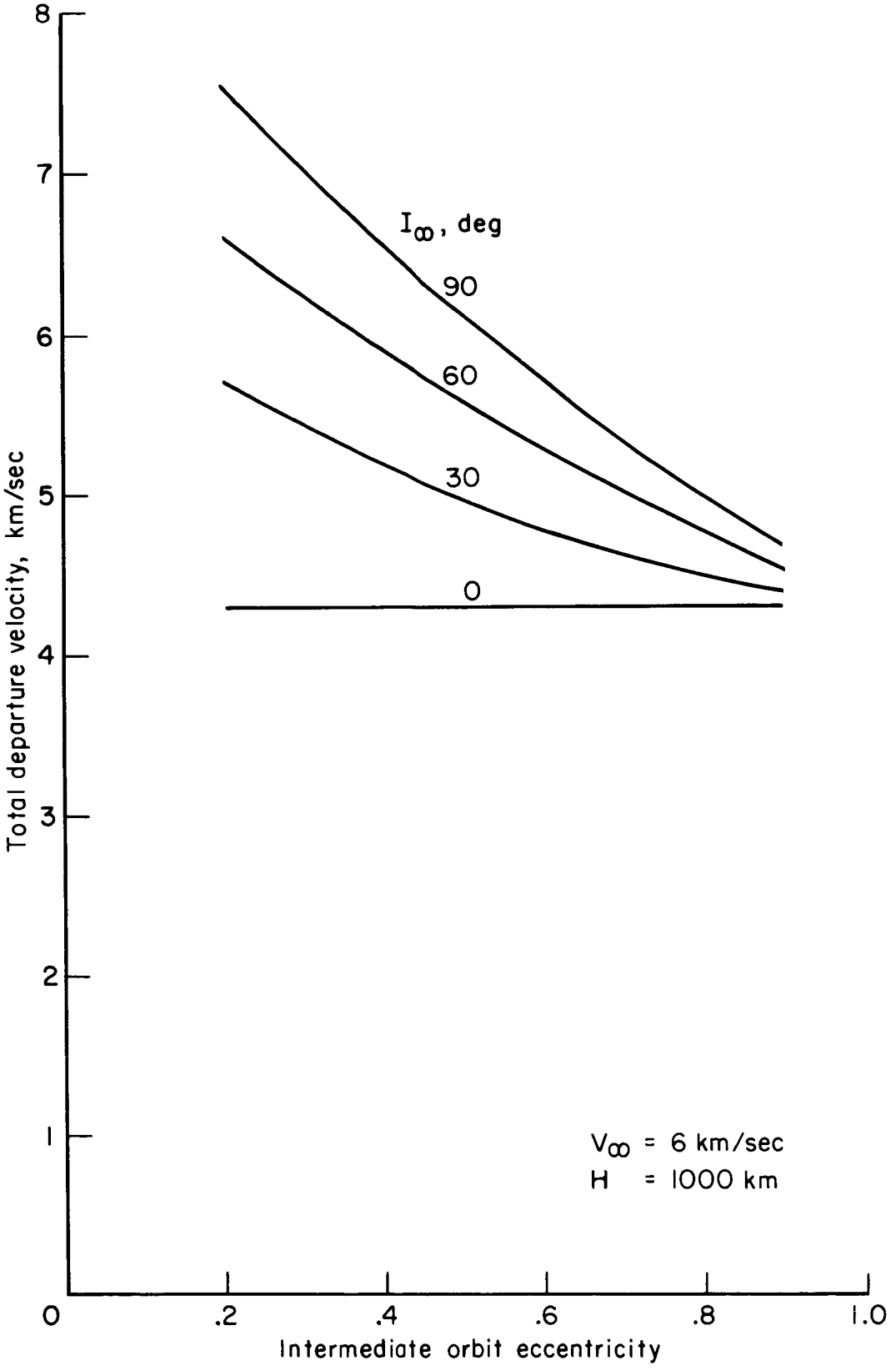

Figure 6(b).

NATIONAL AERONAUTICS AND SPACE ADMINISTRATION
AMES RESEARCH CENTER, MOFFETT FIELD, CALIFORNIA

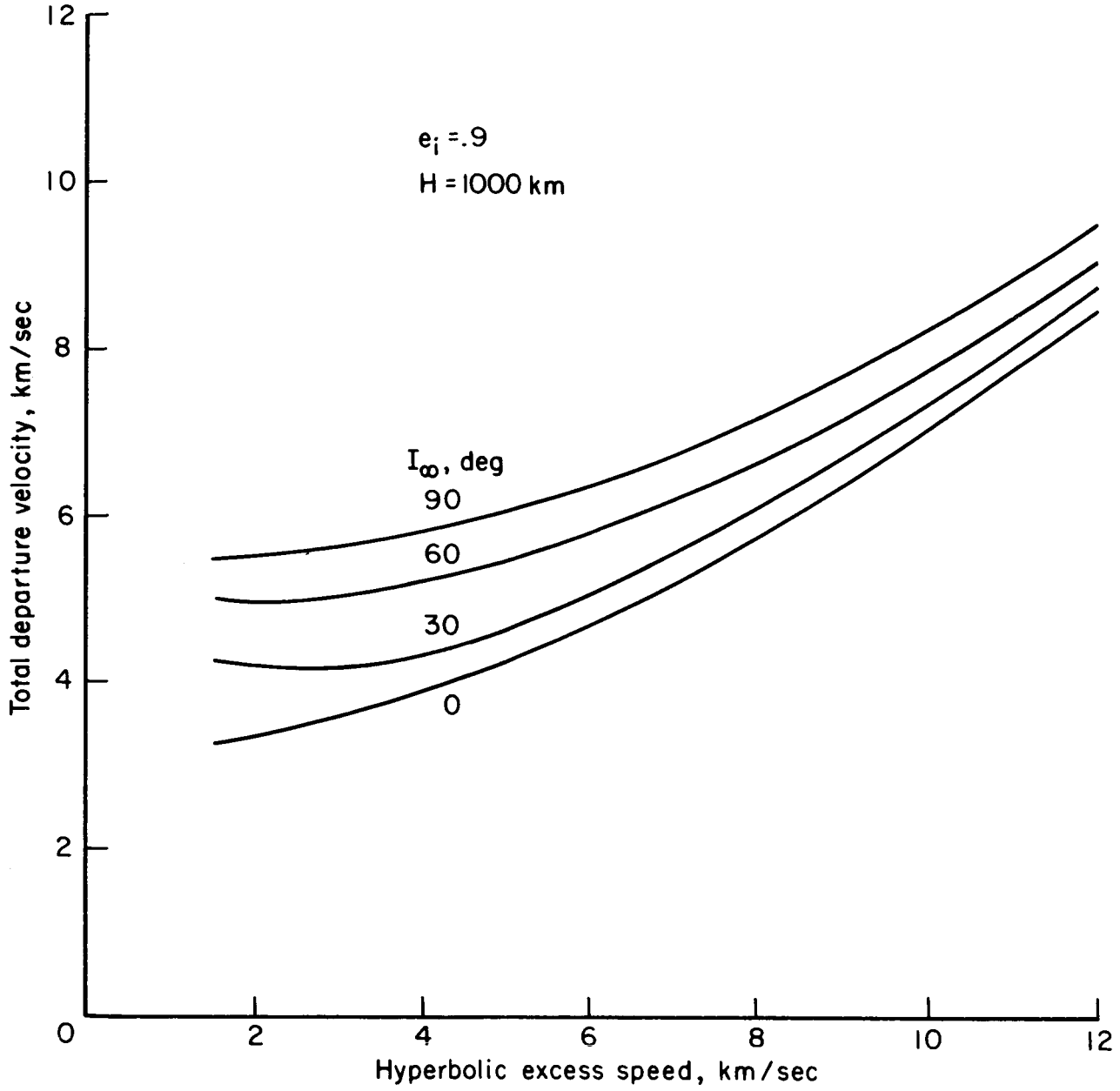

Figure 7(a).

NATIONAL AERONAUTICS AND SPACE ADMINISTRATION
AMES RESEARCH CENTER, MOFFETT FIELD, CALIFORNIA

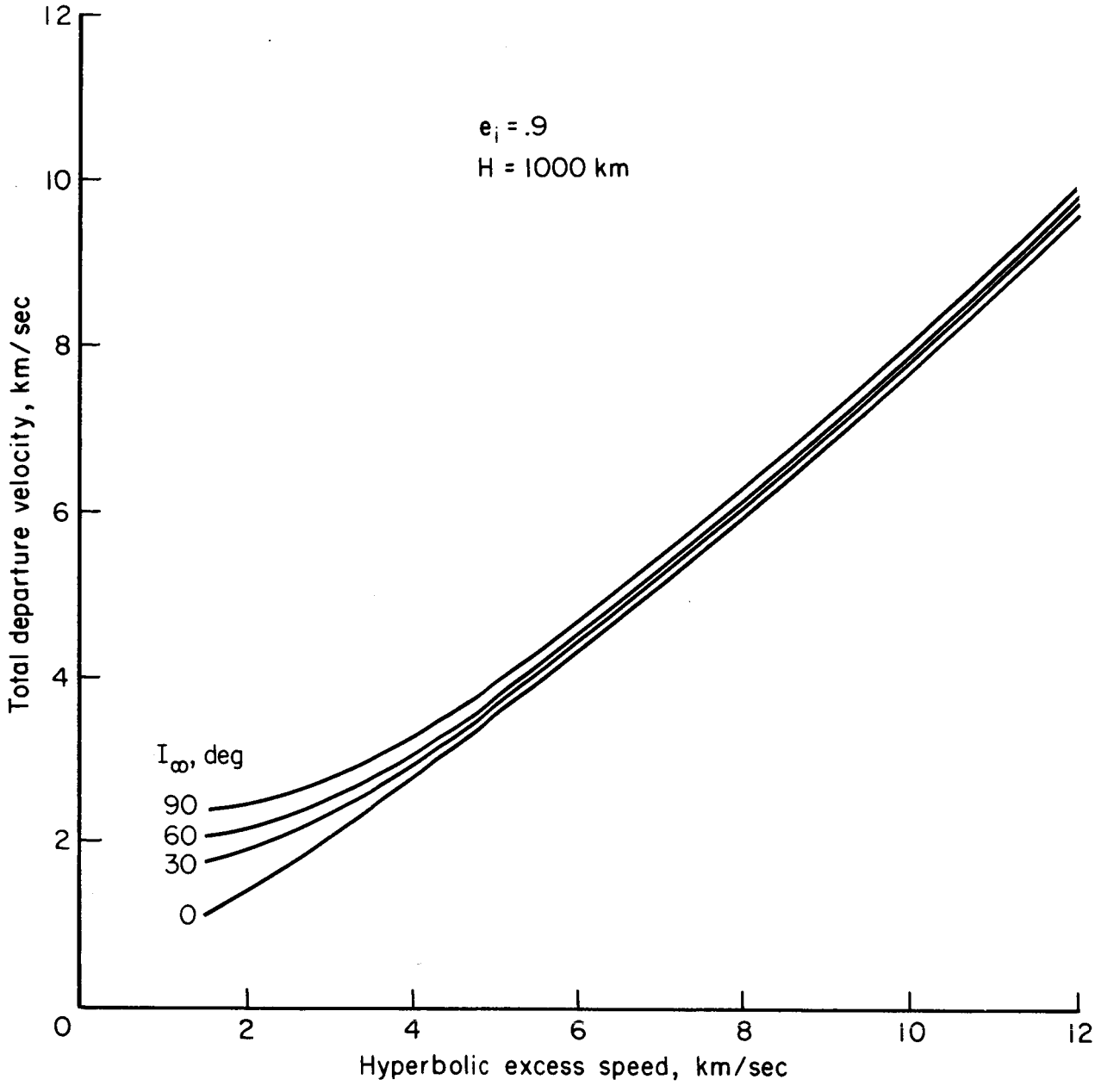

Figure 7(b).

NATIONAL AERONAUTICS AND SPACE ADMINISTRATION
AMES RESEARCH CENTER, MOFFETT FIELD, CALIFORNIA

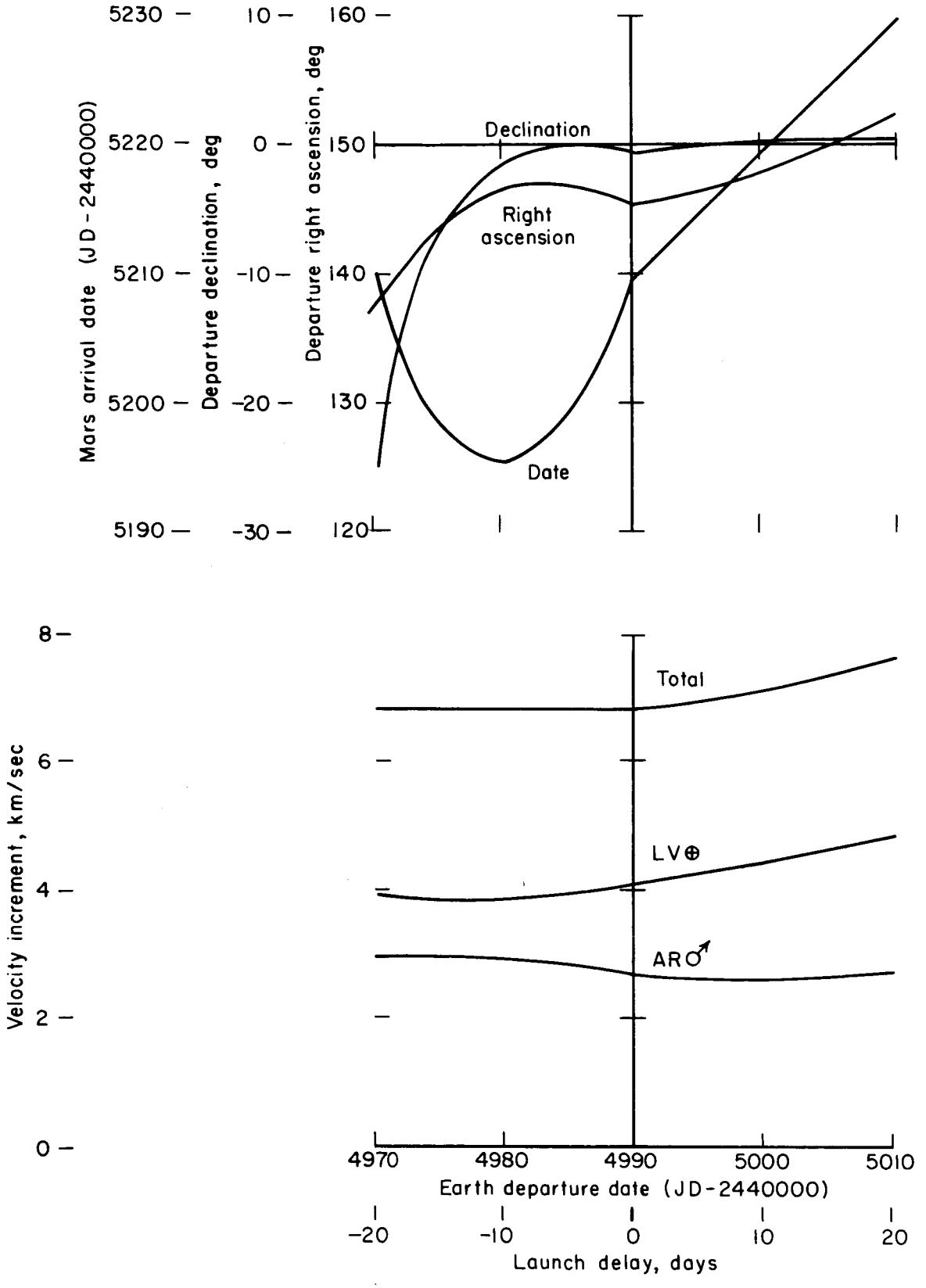

Figure 8(a).

NATIONAL AERONAUTICS AND SPACE ADMINISTRATION
AMES RESEARCH CENTER, MOFFETT FIELD, CALIFORNIA

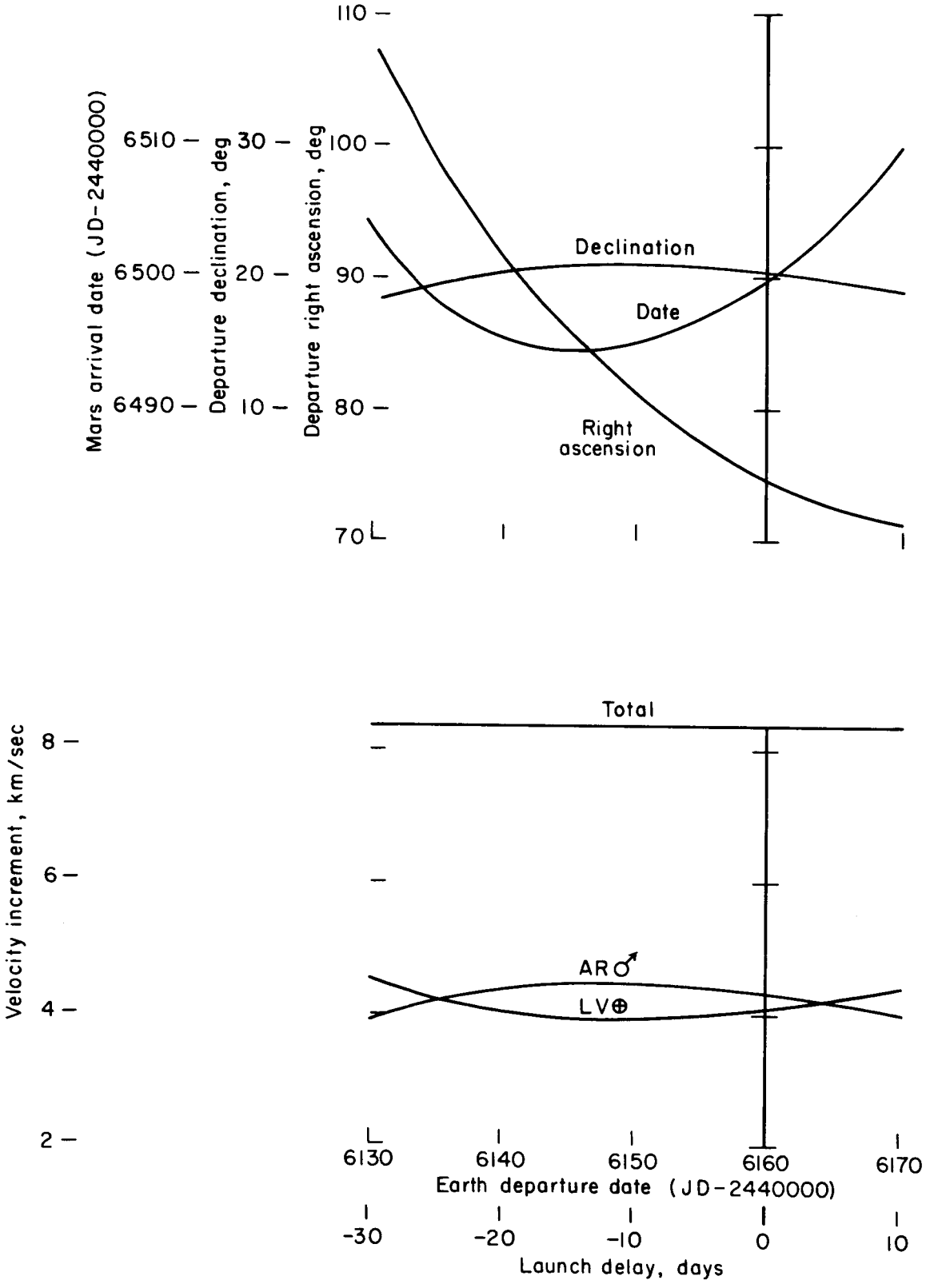

Figure 8(b).

NATIONAL AERONAUTICS AND SPACE ADMINISTRATION
AMES RESEARCH CENTER, MOFFETT FIELD, CALIFORNIA

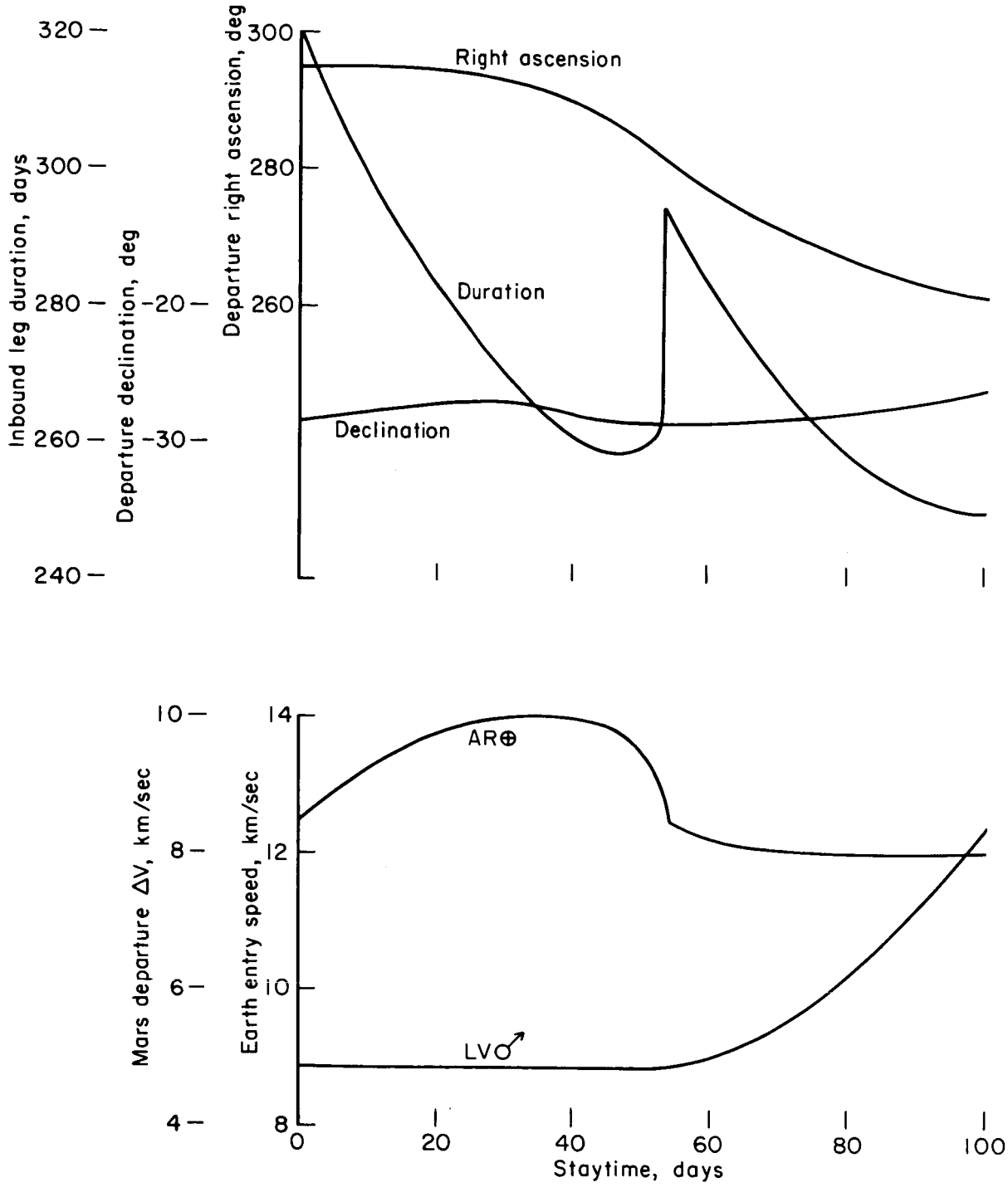
Inbound leg duration, days
320
300
280
260
240
Departure declination, deg
-20
-30
Departure right ascension, deg
300
280
260
Right ascension
Duration
Declination
Mars departure ΔV, km/sec
10
8
6
4
Earth entry speed, km/sec
14
12
10
8
AR⊕
LV♂
0
20
40
60
80
100
Staytime, days

Figure 9(a).

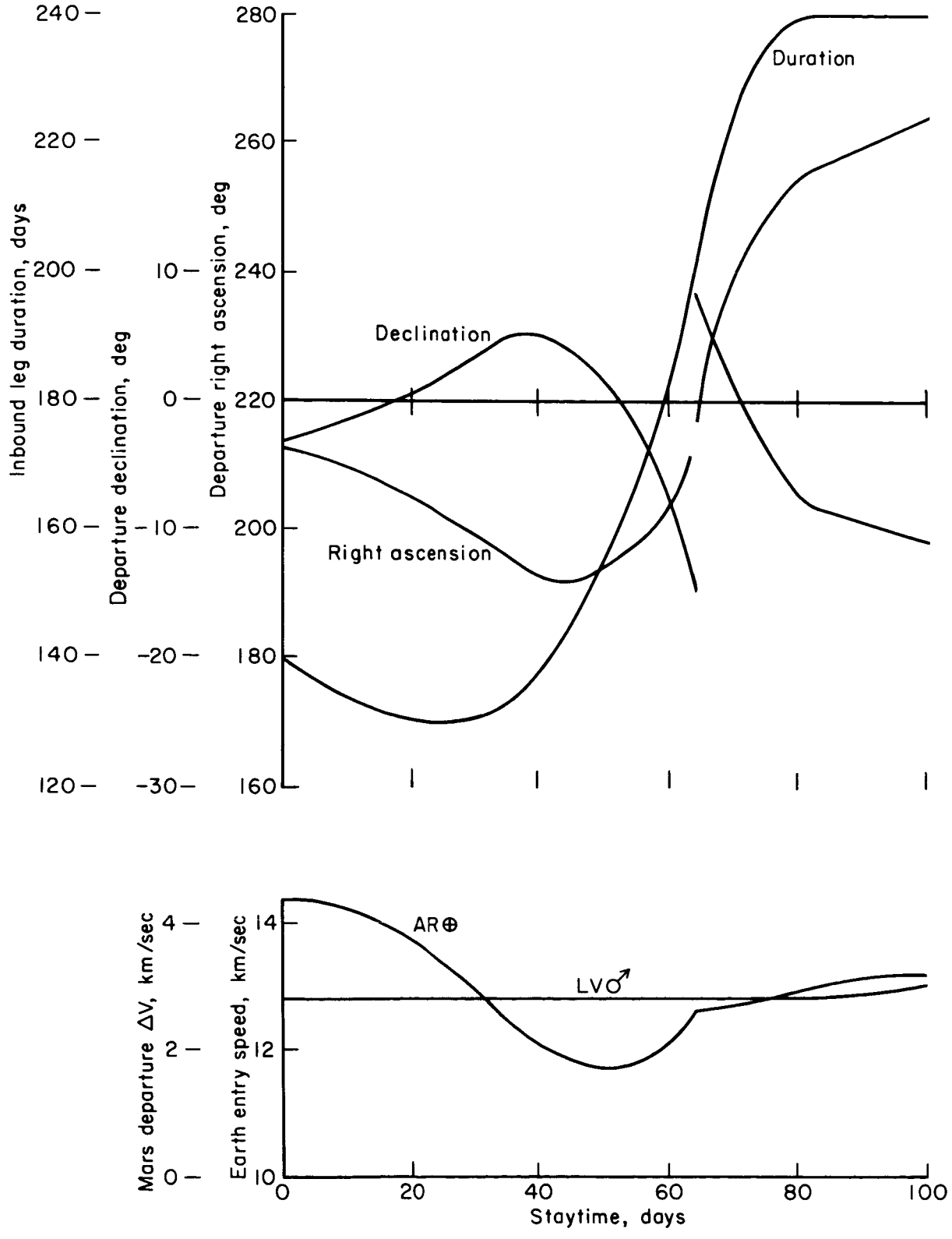
240
220
200
180
160
140
120
Inbound leg duration, days
10
0
-10
-20
-30
Departure declination, deg
280
260
240
220
200
180
160
Departure right ascension, deg
Duration
Declination
Right ascension
4
2
0
Mars departure ΔV, km/sec
14
12
10
Earth entry speed, km/sec
AR⊕
LV♂
0
20
40
60
80
100
Staytime, days

Figure 9(b).

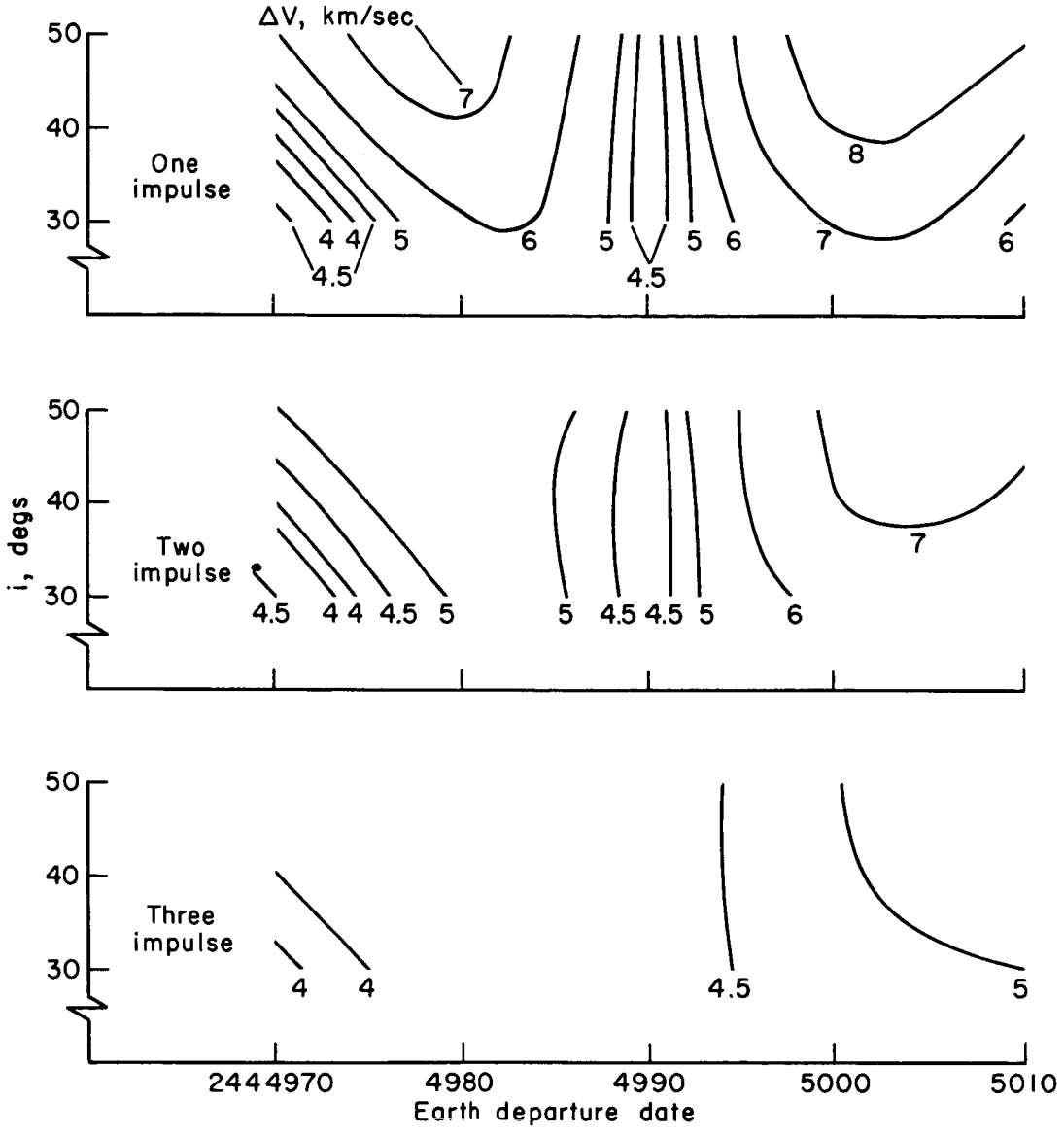
ΔV, km/sec
50
40
30
One impulse
7
8
4 4
5
6
5
5
6
7
6
4.5
4.5
i, degs
Two impulse
4.5
4 4
4.5
5
5
4.5
4.5
5
6
7
Three impulse
4
4
4.5
5
2444970
4980
4990
5000
5010
Earth departure date

Figure 10(a).

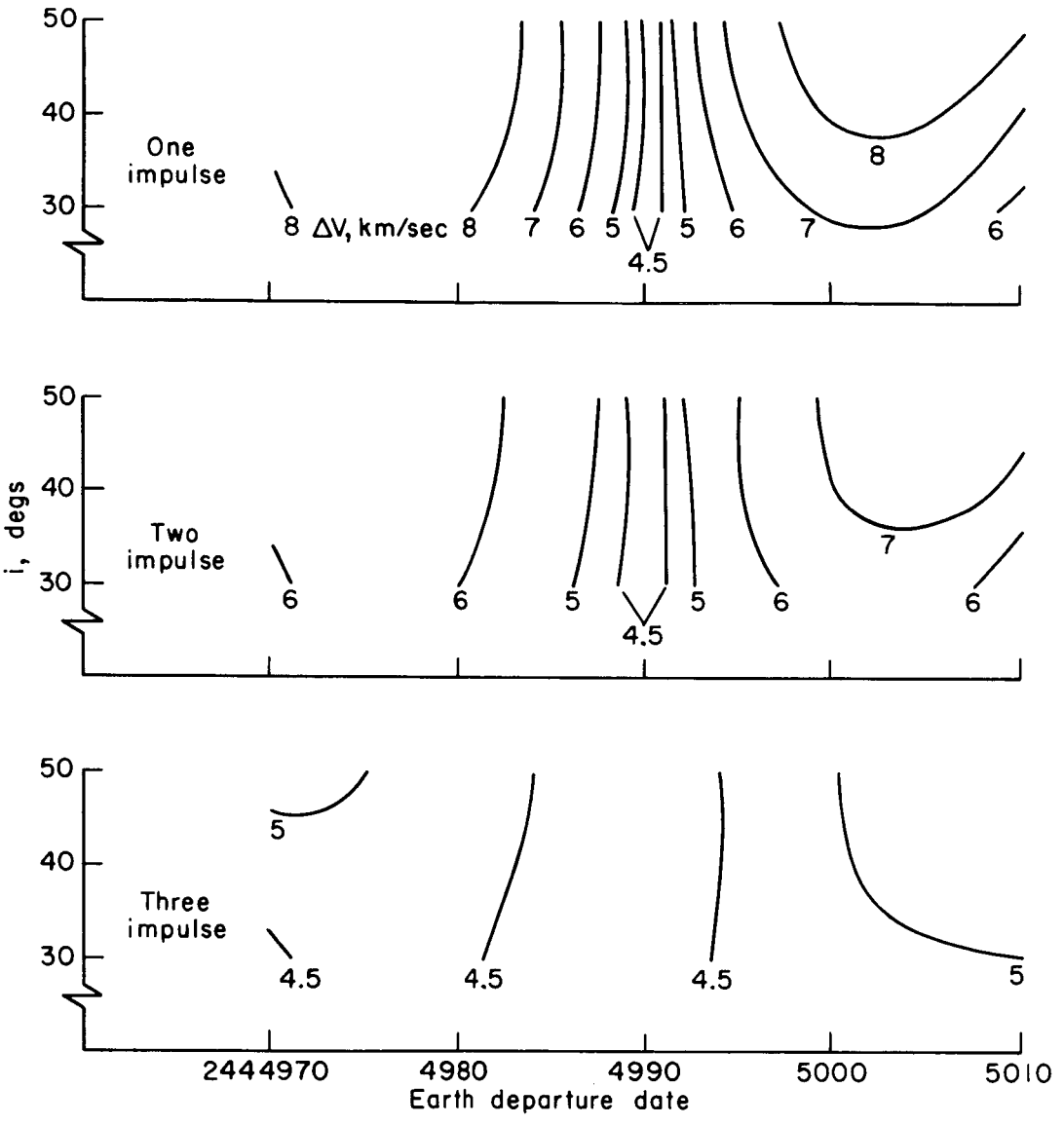
50
40
30
One impulse
8 ΔV, km/sec 8 7 6 5 4.5 5 6 7 8 6
Two impulse
6 6 5 4.5 5 6 7 6
Three impulse
5 4.5 4.5 4.5 5
i, degs
2444970
4980
4990
5000
5010
Earth departure date

Figure 10(b).

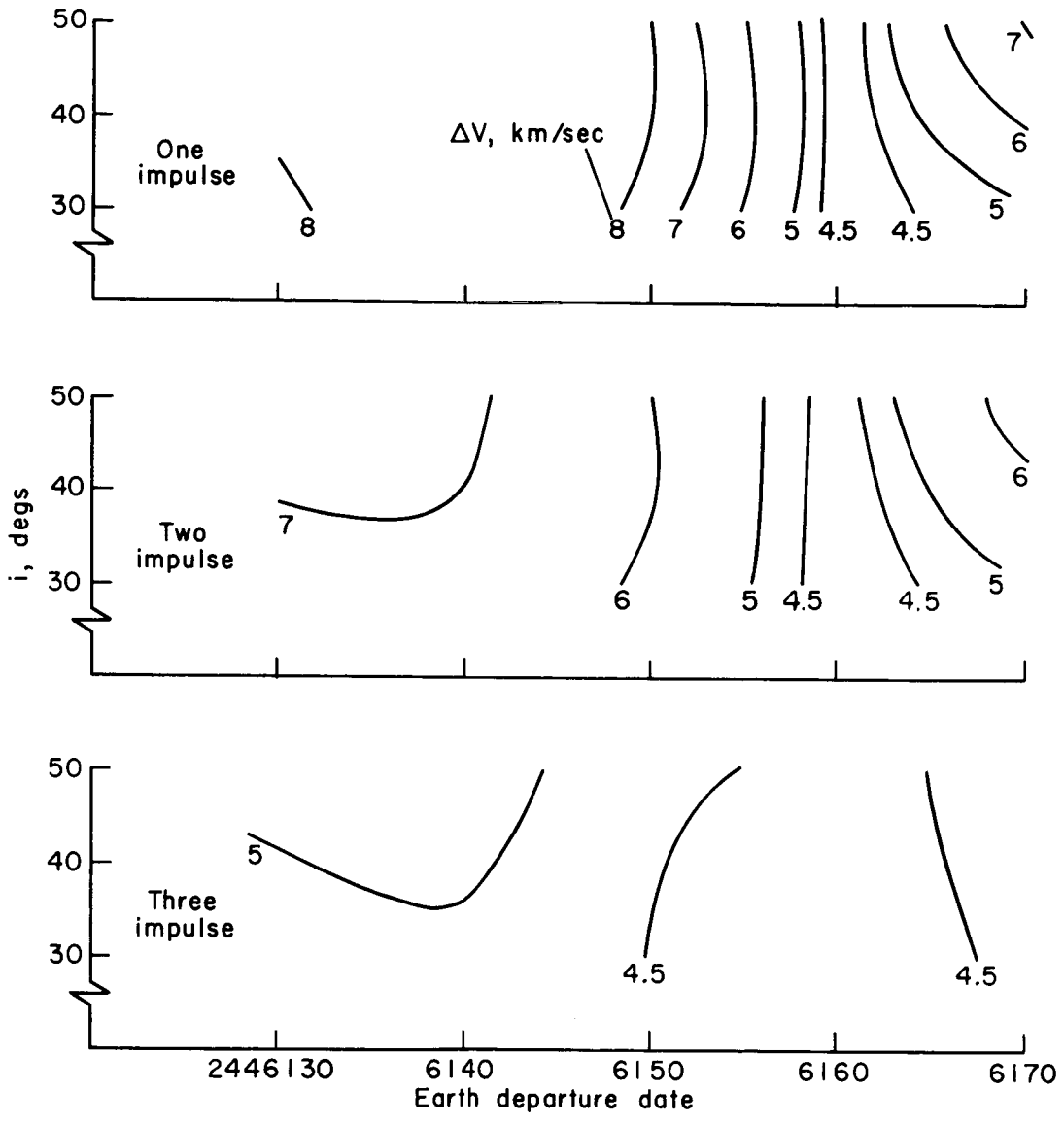
50
40
30
One impulse
ΔV, km/sec
8
8
7
6
5
4.5
4.5
7
6
5
Two impulse
7
6
5
4.5
4.5
6
5
Three impulse
5
4.5
4.5
i, degs
2446130
6140
6150
6160
6170
Earth departure date

Figure 11(a).

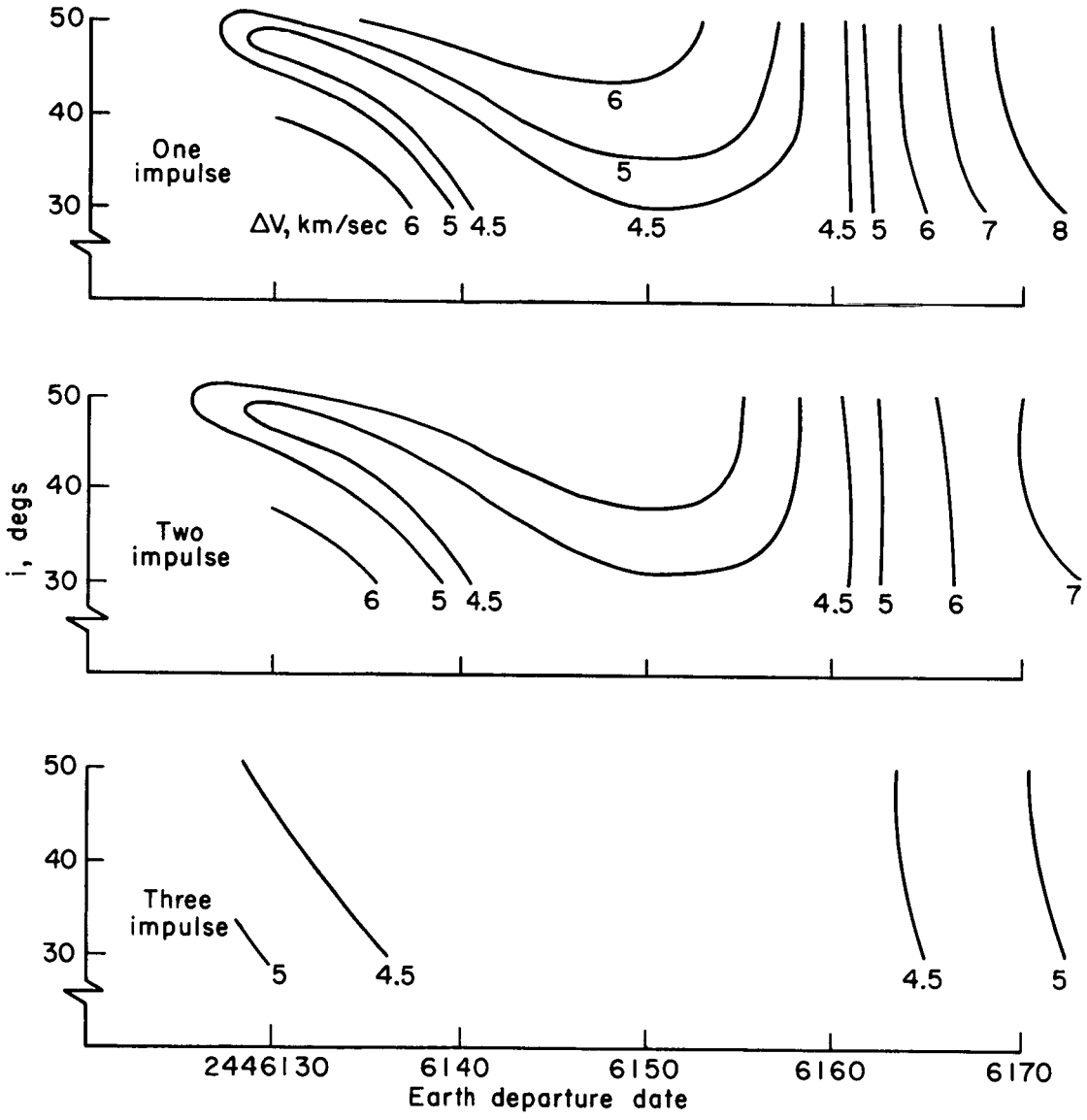
50
40
30
One impulse
ΔV, km/sec 6 5 4.5
6
5
4.5
4.5 5 6 7 8
i, degs
Two impulse
6 5 4.5
4.5 5 6 7
Three impulse
5
4.5
4.5 5
2446130
6140
6150
6160
6170
Earth departure date

Figure 11(b).

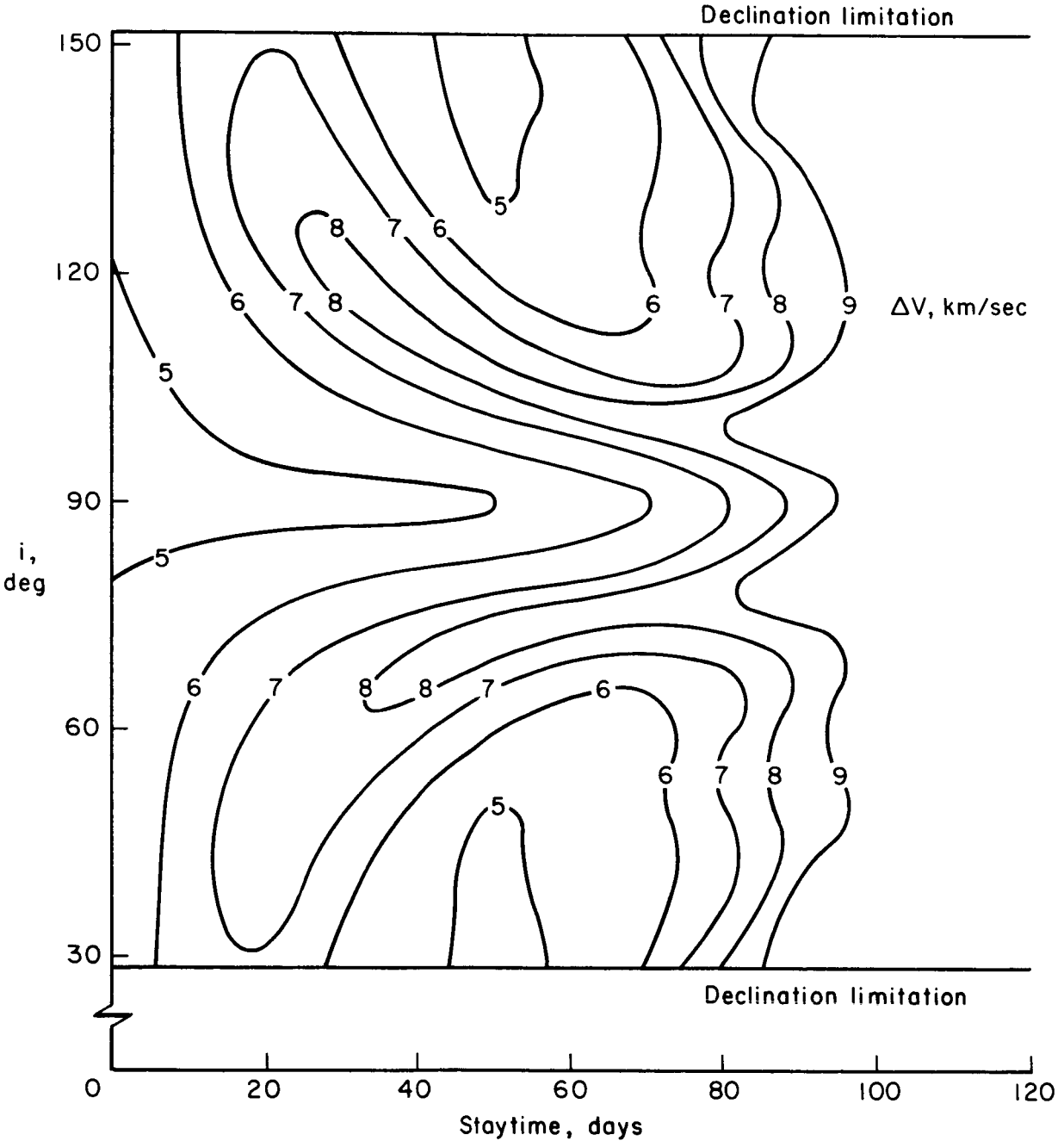
Declination limitation
150
120
90
60
30
0
i,
deg
ΔV, km/sec
Declination limitation
20
40
60
80
100
120
Staytime, days

Figure 12(a).

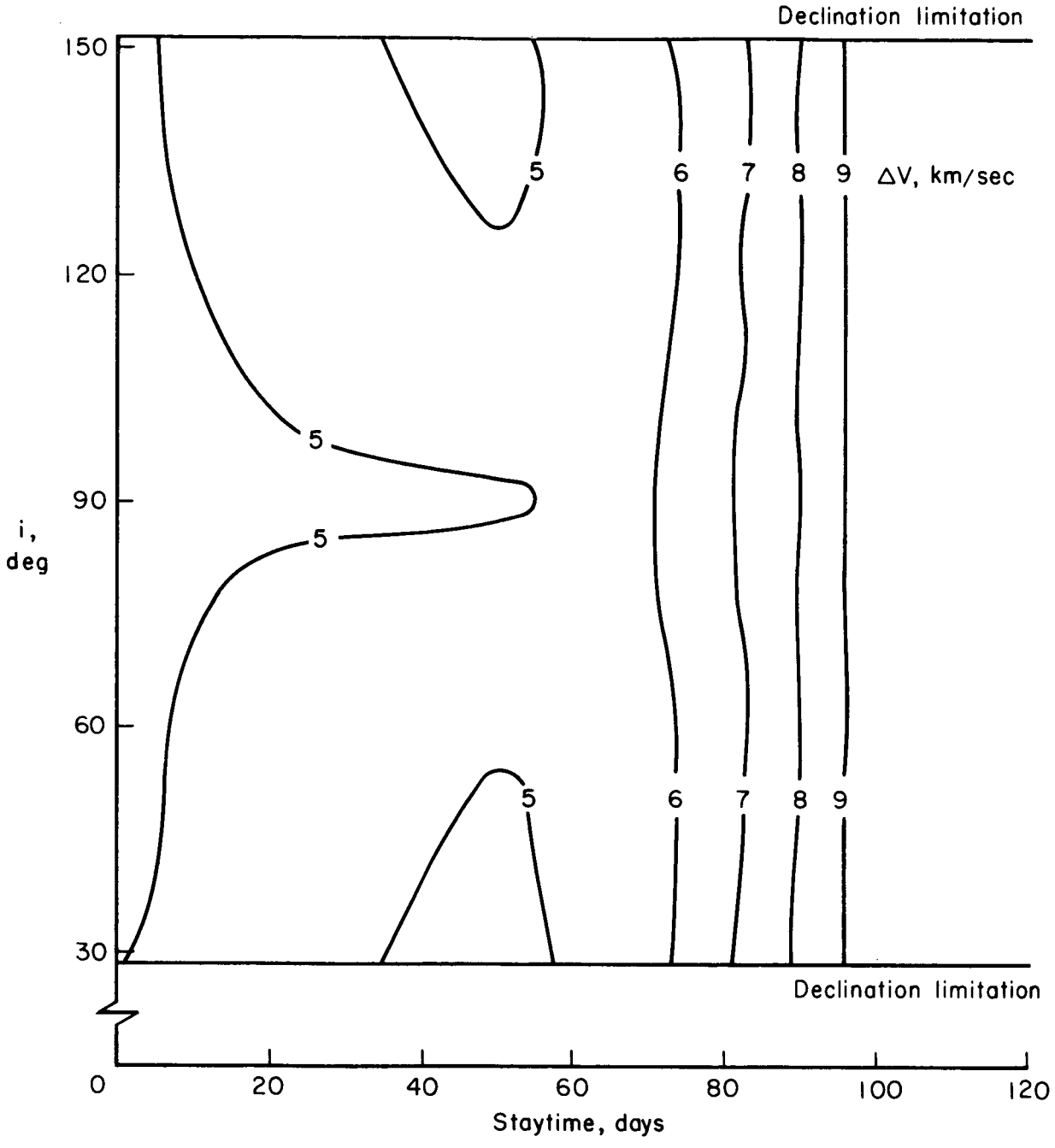
Declination limitation
150
120
90
60
30
i,
deg
5
5
5
6
7
8
9
ΔV, km/sec
6
7
8
9
Declination limitation
0
20
40
60
80
100
120
Staytime, days

Figure 12(b).

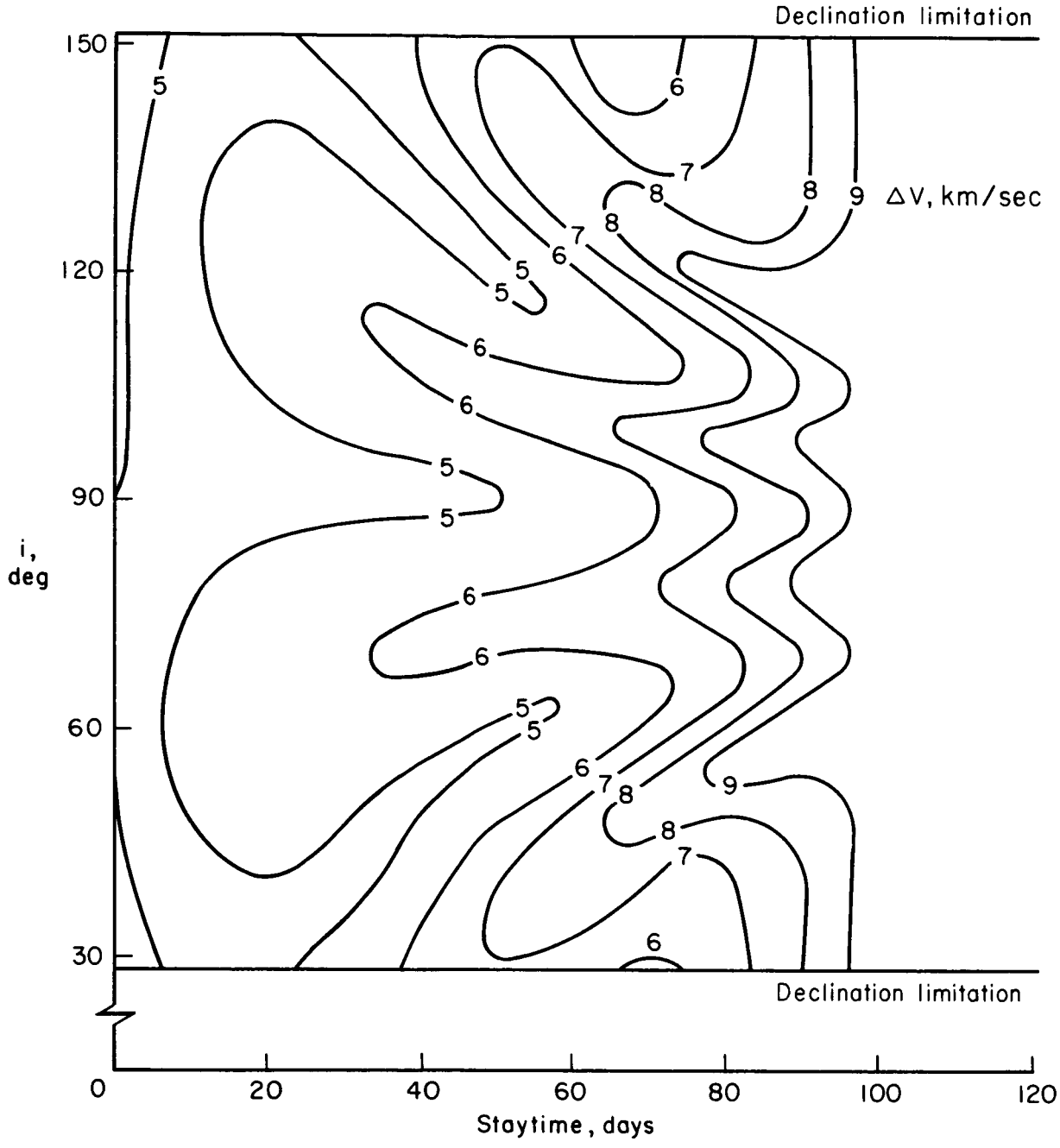
Declination limitation
150
120
90
60
30
i,
deg
5
6
7
8
9
ΔV, km/sec
Declination limitation
0
20
40
60
80
100
120
Staytime, days

Figure 12(c)

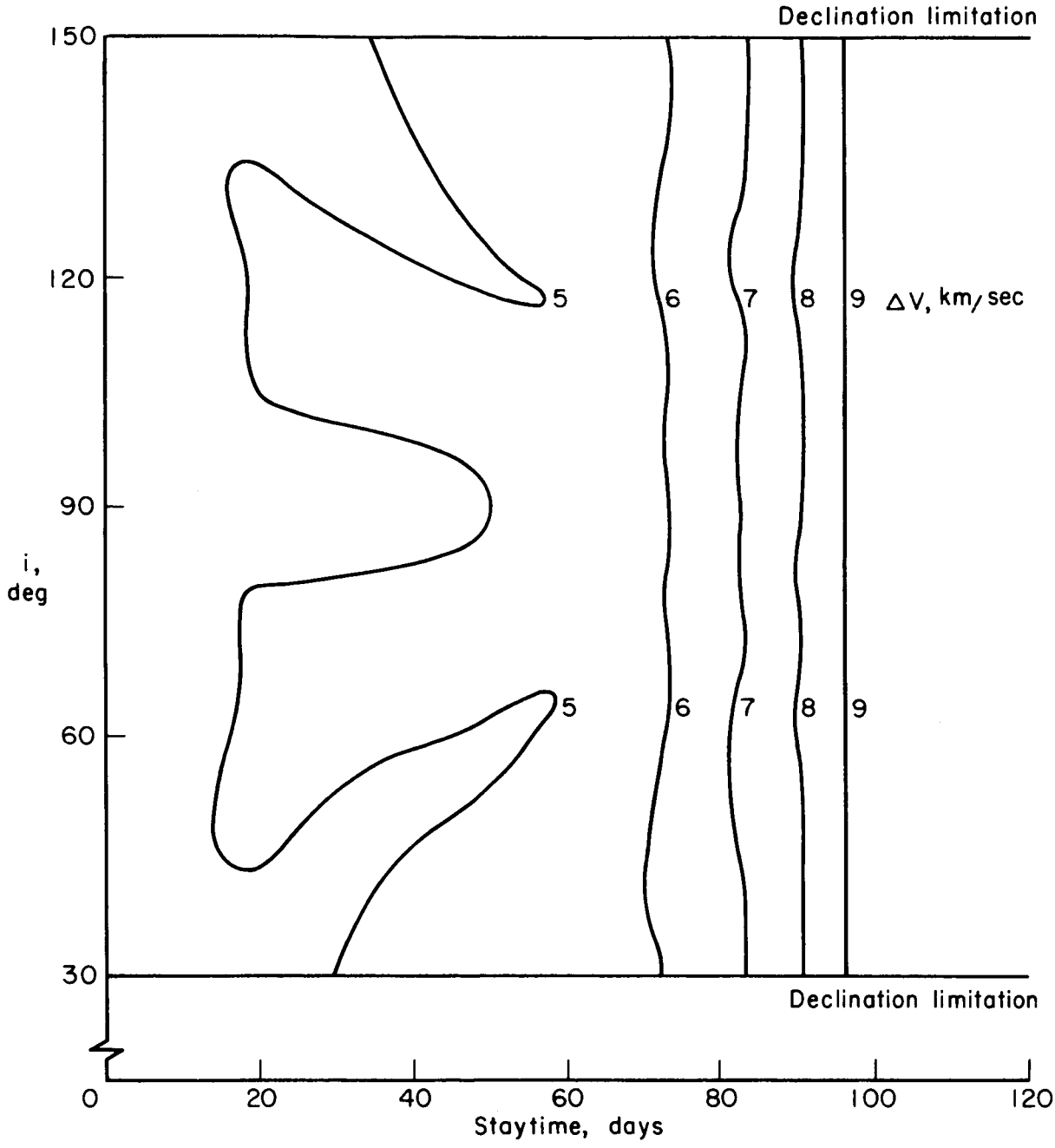
Declination limitation
150
120
90
60
30
i,
deg
5
6
7
8
9
ΔV, km/sec
5
6
7
8
9
Declination limitation
0
20
40
60
80
100
120
Staytime, days

Figure 12(d)

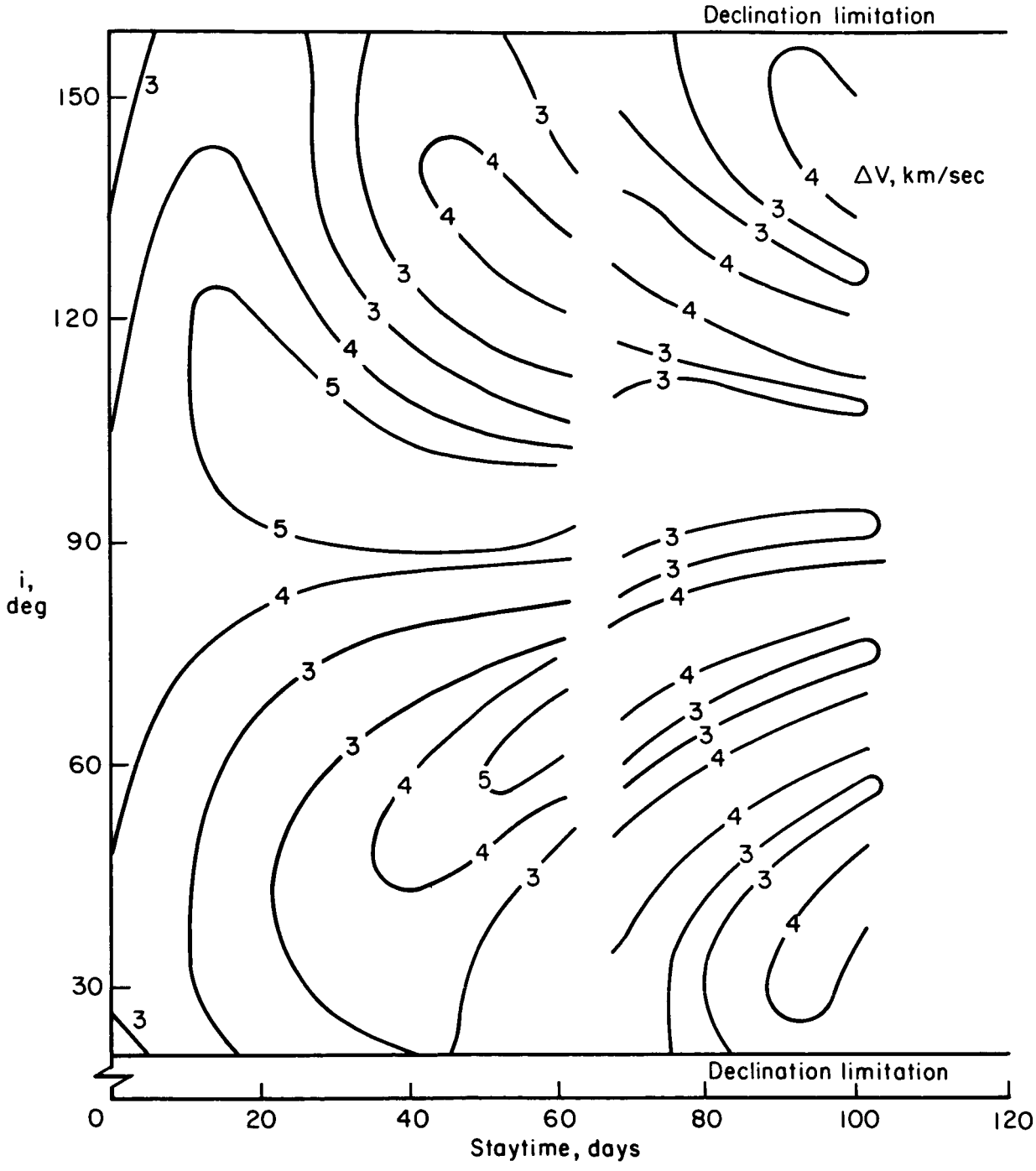
Declination limitation
ΔV, km/sec
150
120
90
60
30
i, deg
Declination limitation
0
20
40
60
80
100
120
Staytime, days

Figure 13(a).

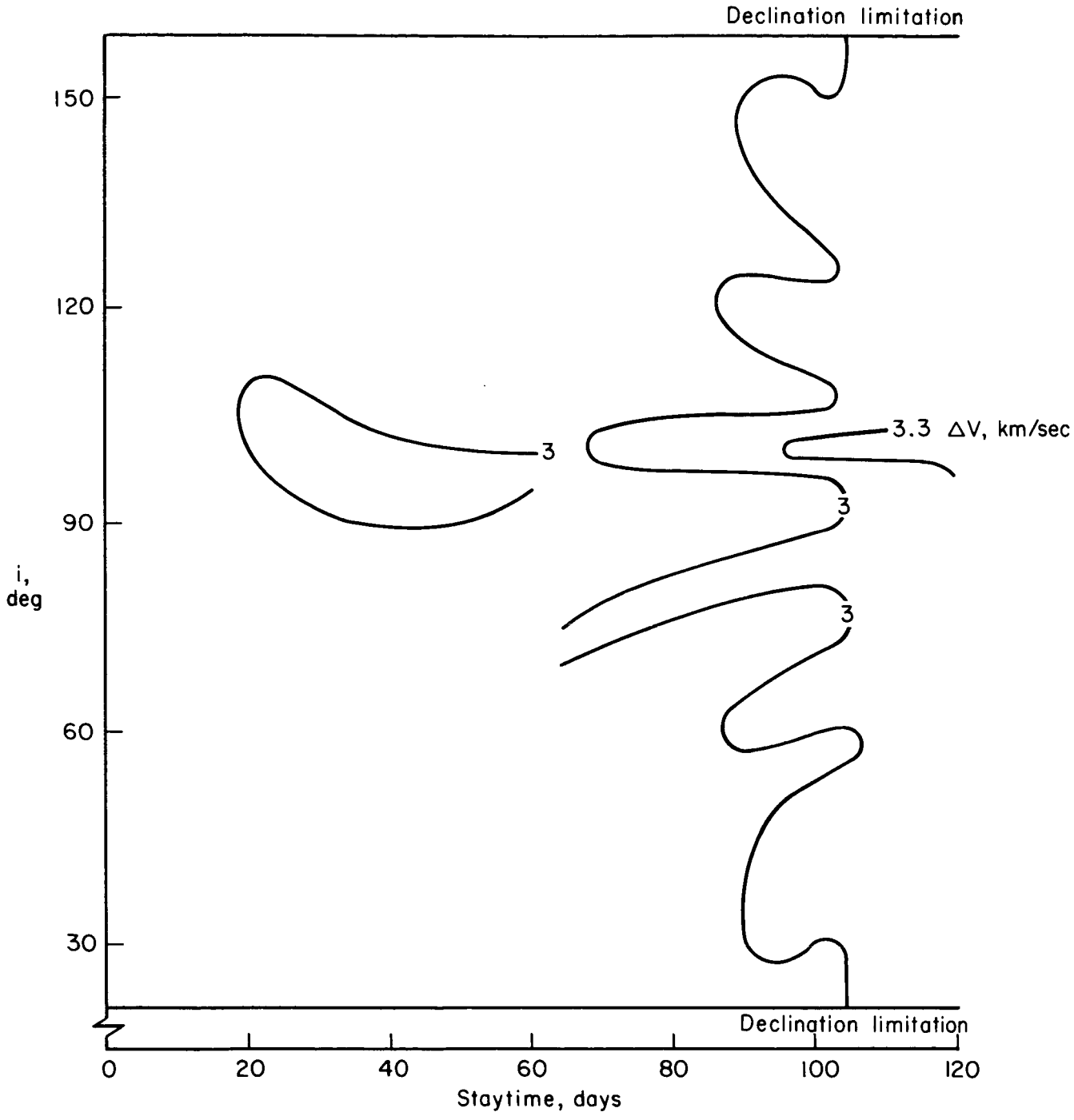
Declination limitation
150
120
90
60
30
i,
deg
3
3
3
3.3 ΔV, km/sec
Declination limitation
0
20
40
60
80
100
120
Staytime, days

Figure 13(b).

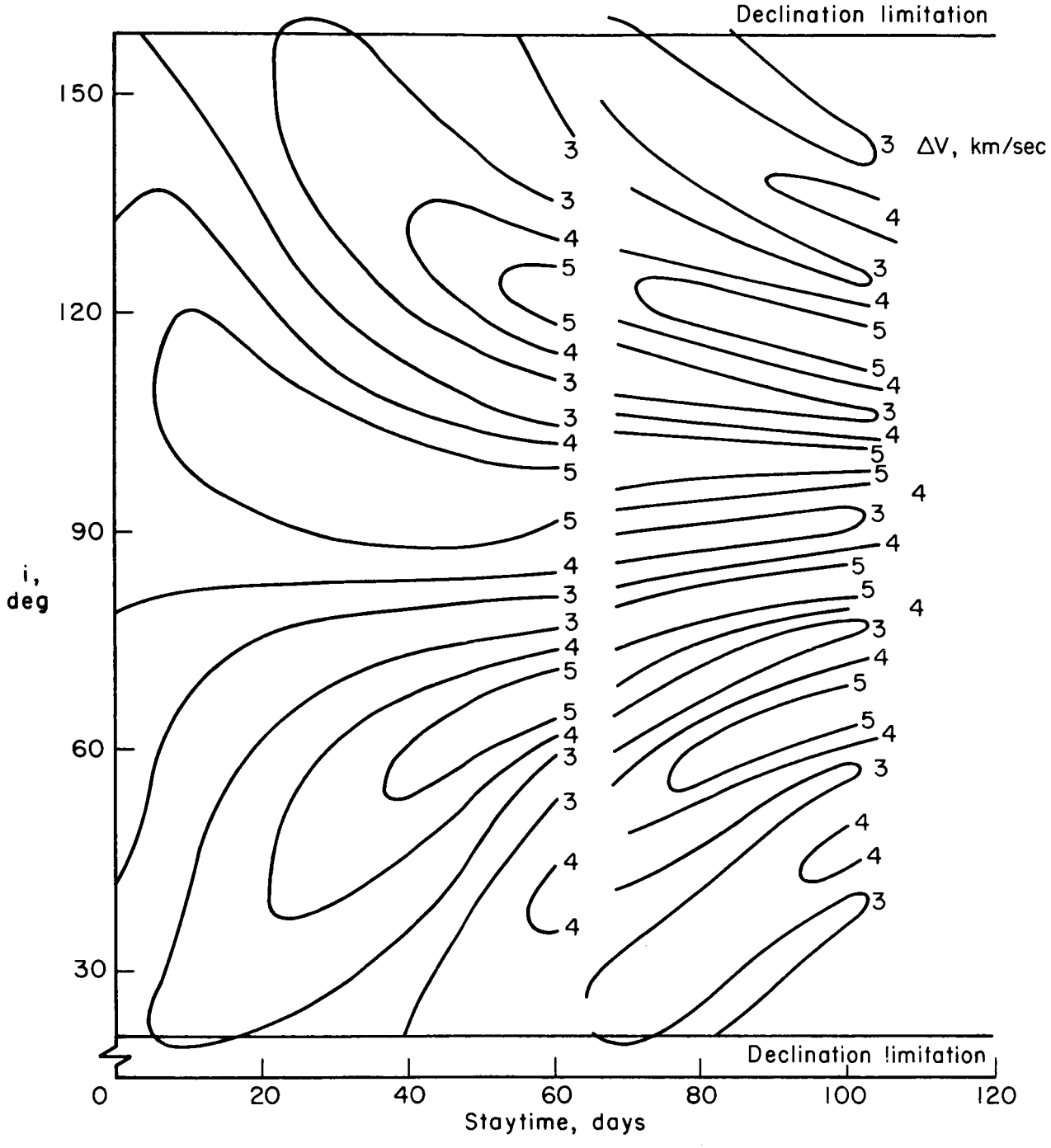

Figure 13(c)

NATIONAL AERONAUTICS AND SPACE ADMINISTRATION
AMES RESEARCH CENTER, MOFFETT FIELD, CALIFORNIA

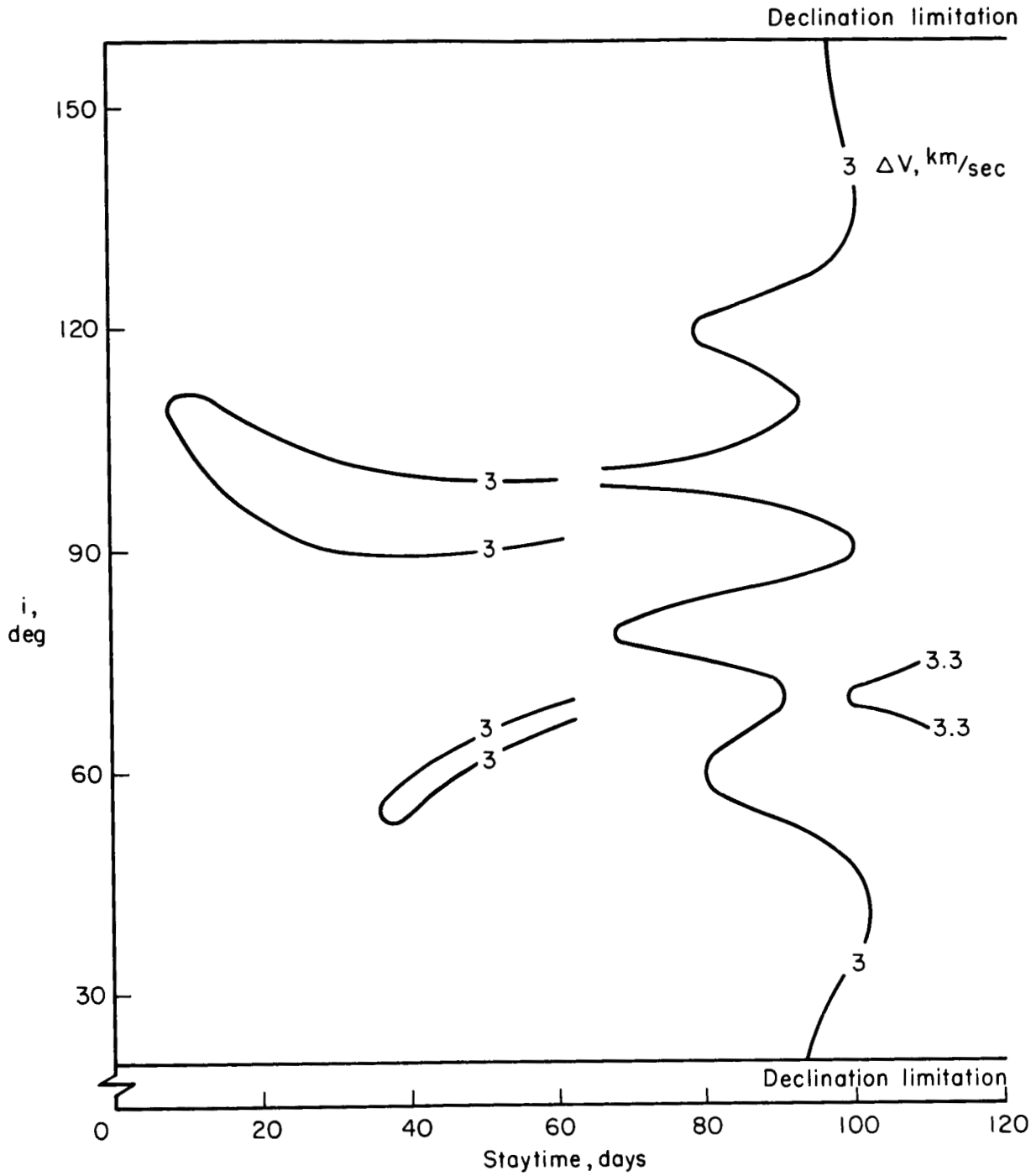

Figure 13(d)

NATIONAL AERONAUTICS AND SPACE ADMINISTRATION
AMES RESEARCH CENTER, MOFFETT FIELD, CALIFORNIA

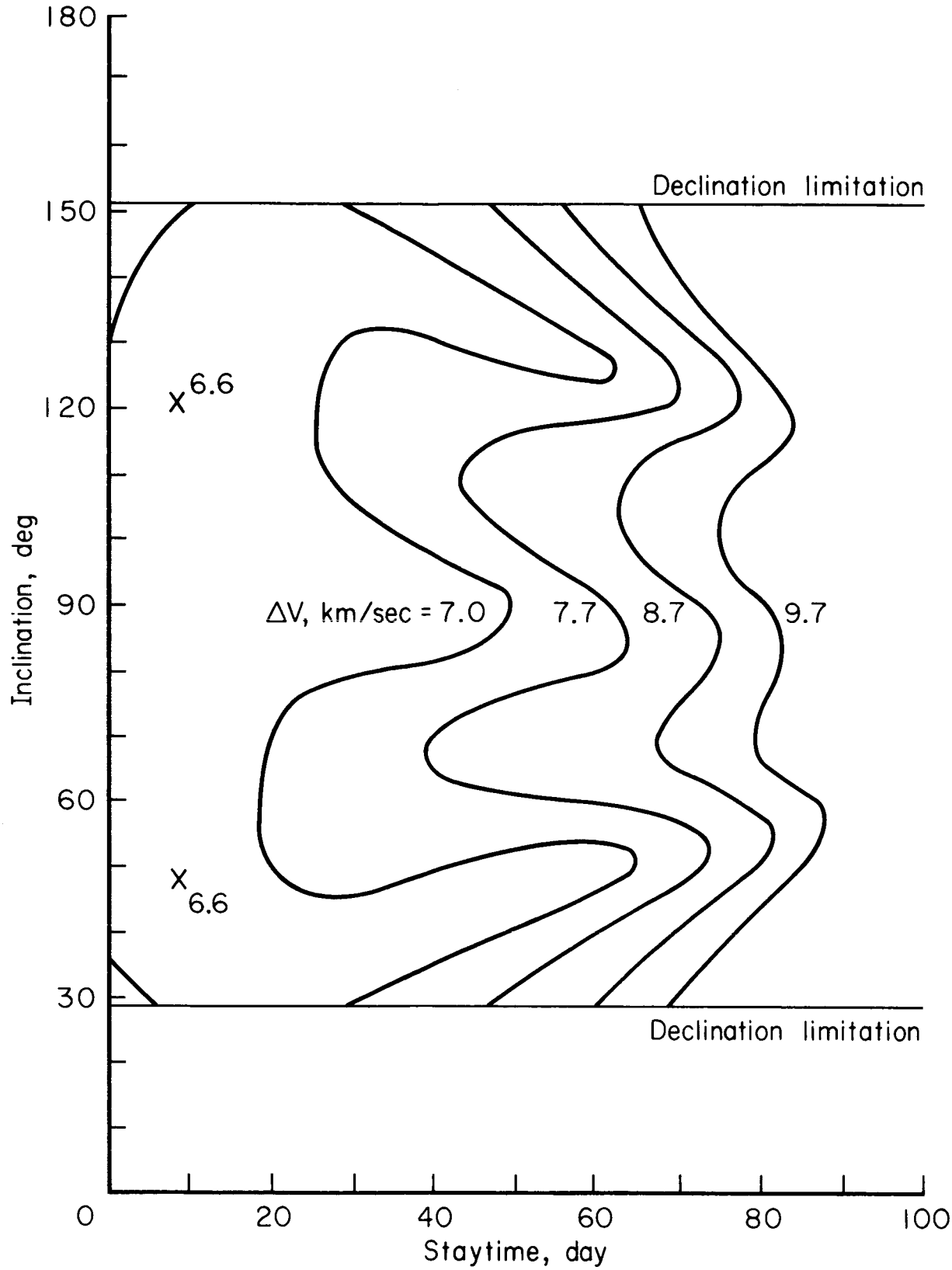

Figure 14(a)

NATIONAL AERONAUTICS AND SPACE ADMINISTRATION
AMES RESEARCH CENTER, MOFFETT FIELD, CALIFORNIA

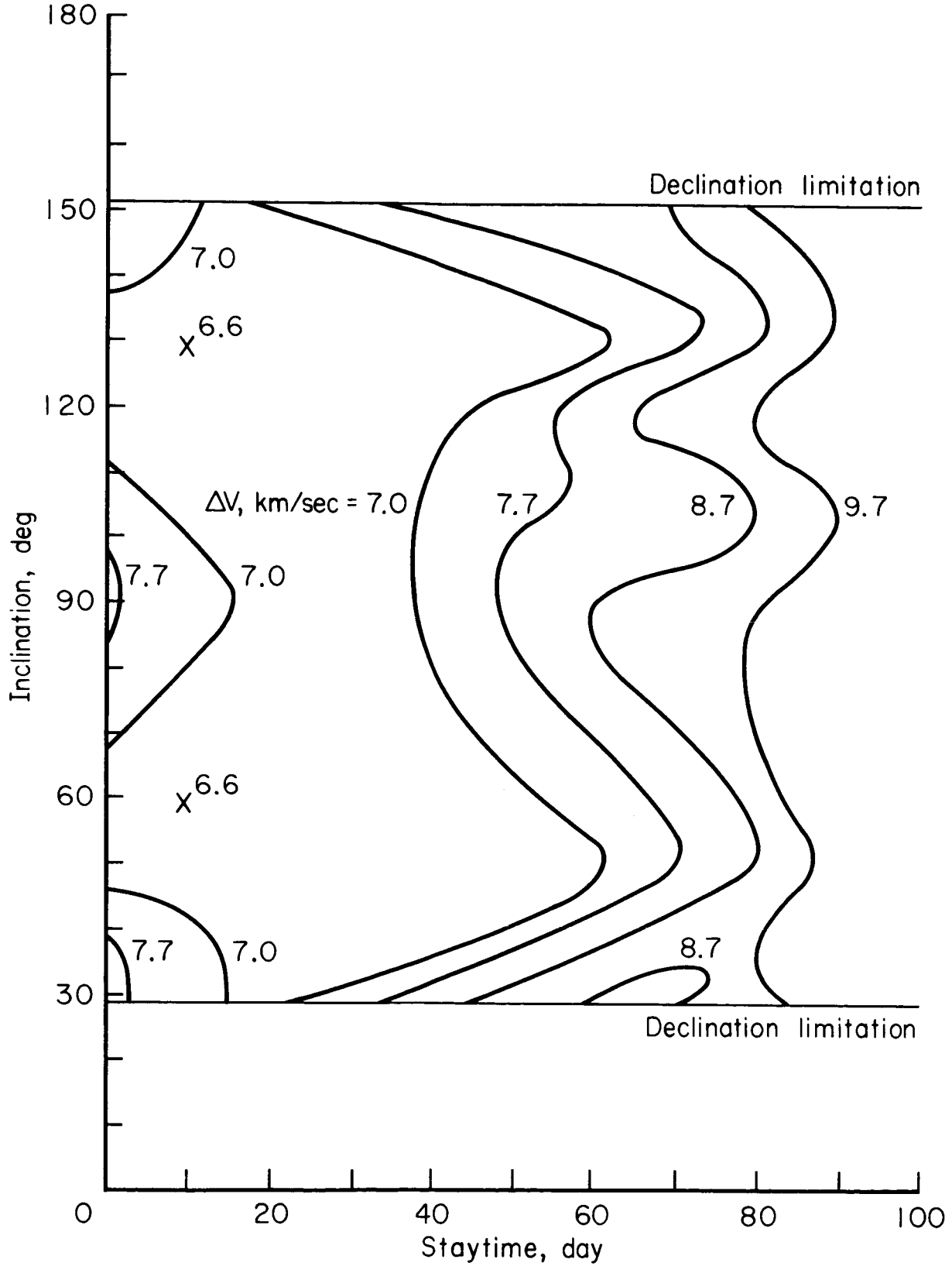

Figure 14(b).

NATIONAL AERONAUTICS AND SPACE ADMINISTRATION
AMES RESEARCH CENTER, MOFFETT FIELD, CALIFORNIA

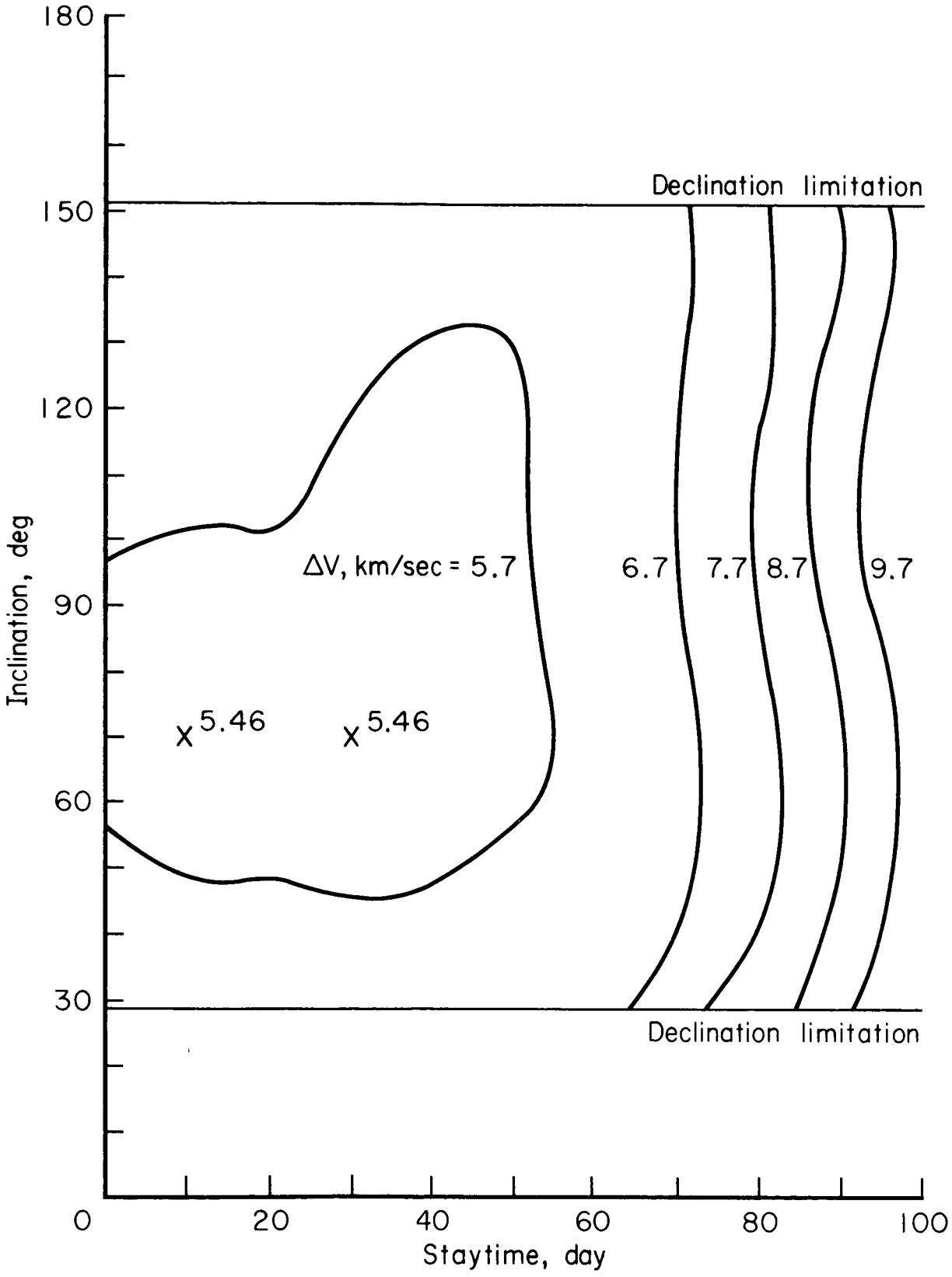

Figure 15.

NATIONAL AERONAUTICS AND SPACE ADMINISTRATION
AMES RESEARCH CENTER, MOFFETT FIELD, CALIFORNIA

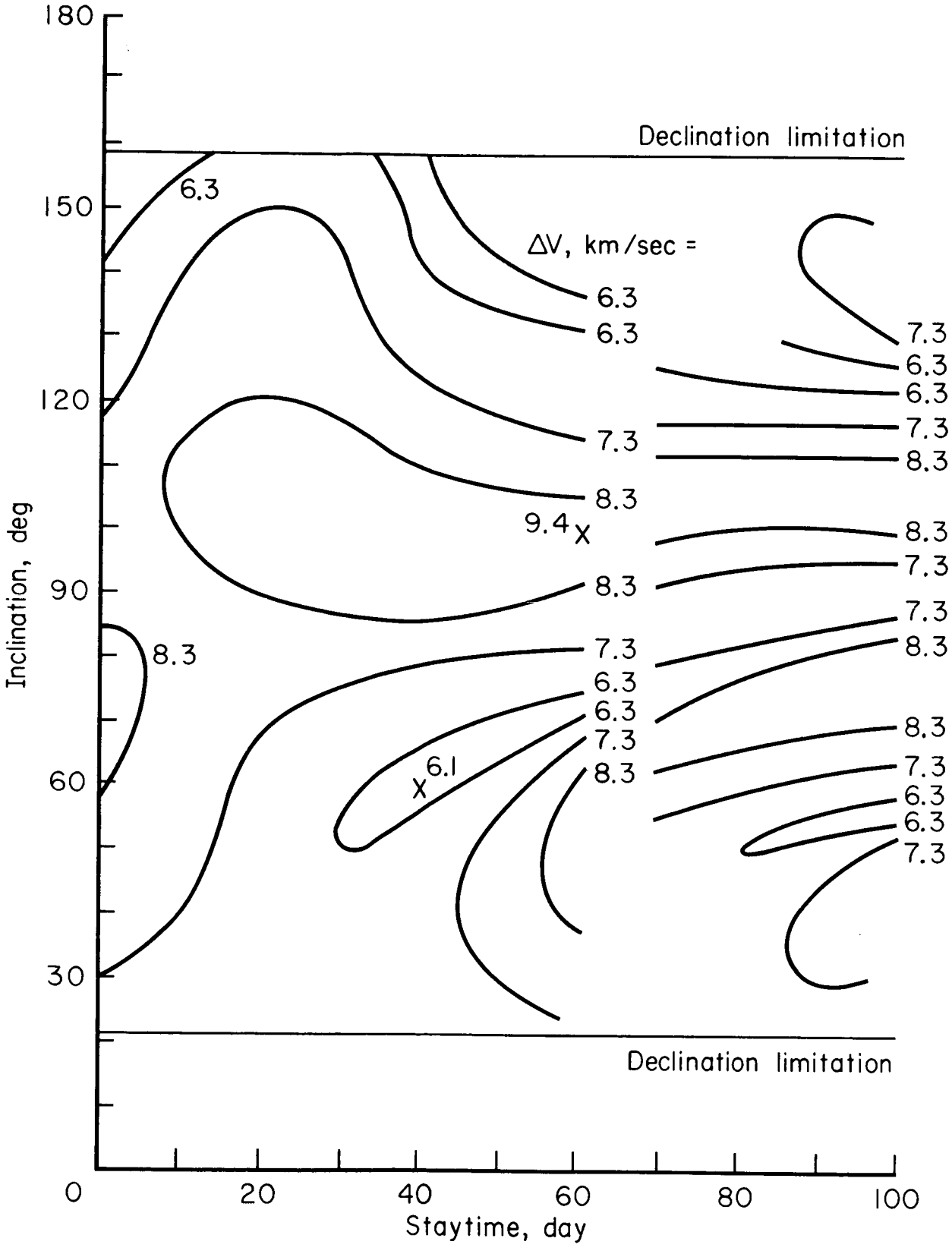

Figure 16(a).

NATIONAL AERONAUTICS AND SPACE ADMINISTRATION
AMES RESEARCH CENTER, MOFFETT FIELD, CALIFORNIA

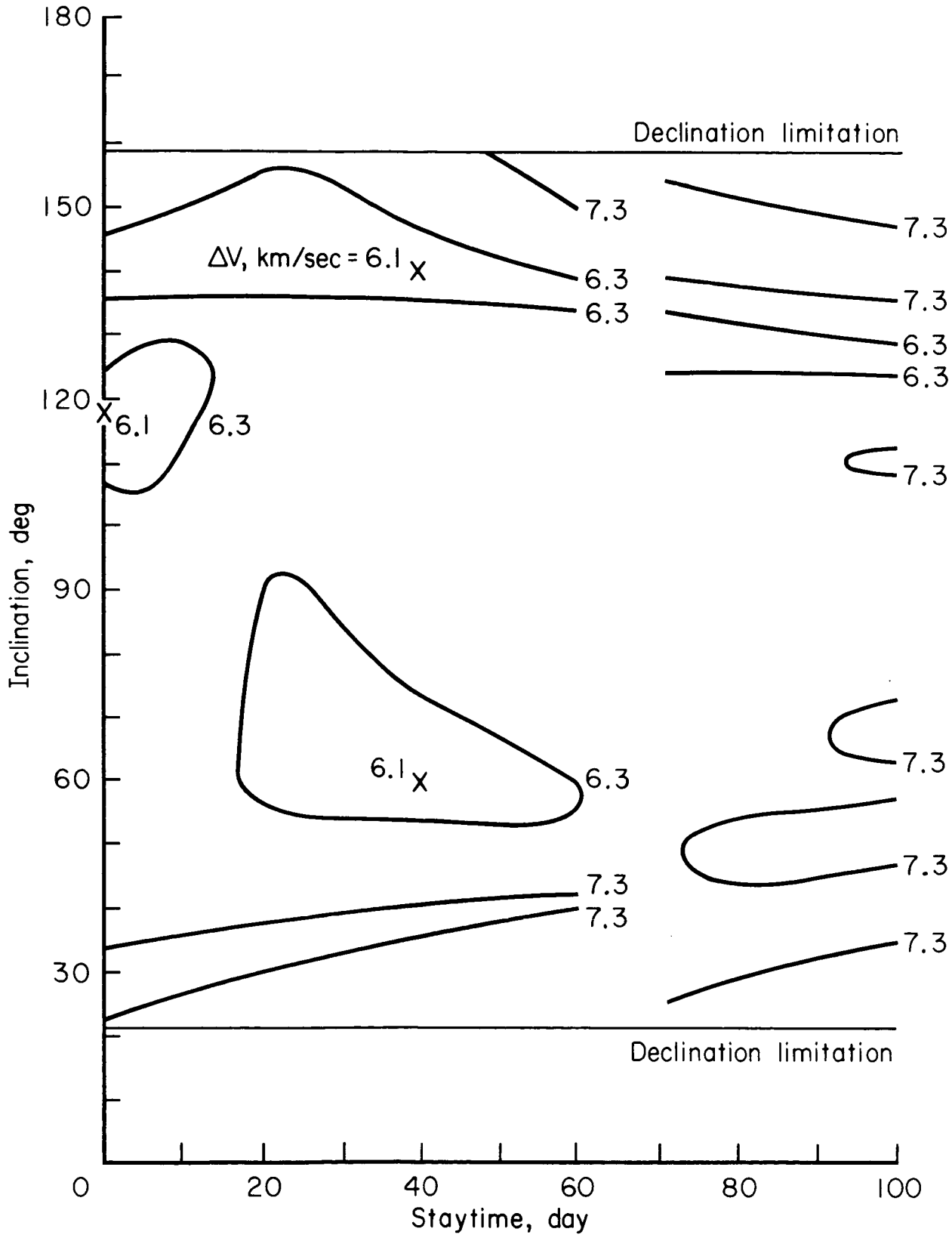

Figure 16(b).

NATIONAL AERONAUTICS AND SPACE ADMINISTRATION
AMES RESEARCH CENTER, MOFFETT FIELD, CALIFORNIA

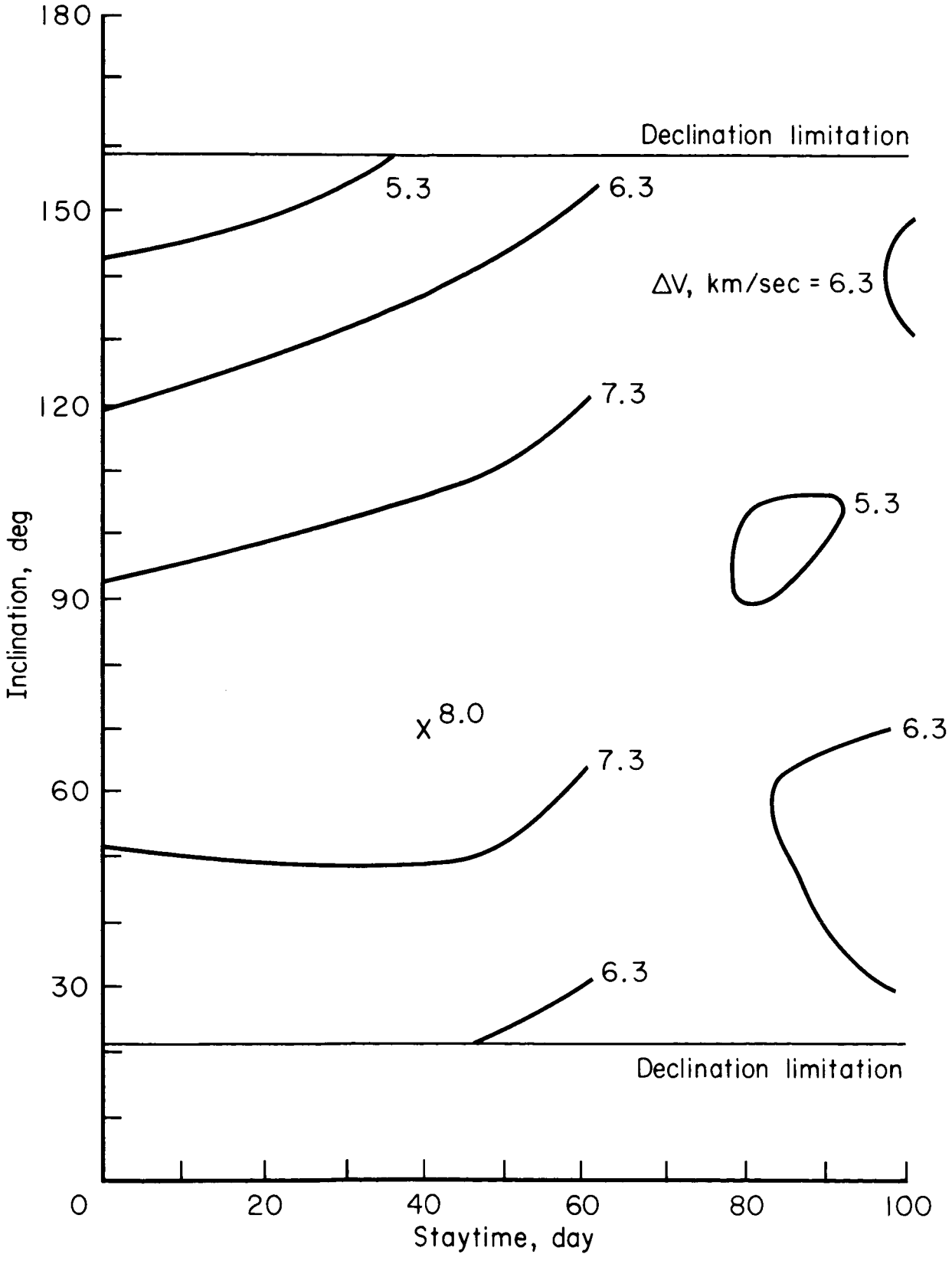

Figure 17(a).

NATIONAL AERONAUTICS AND SPACE ADMINISTRATION
AMES RESEARCH CENTER, MOFFETT FIELD, CALIFORNIA

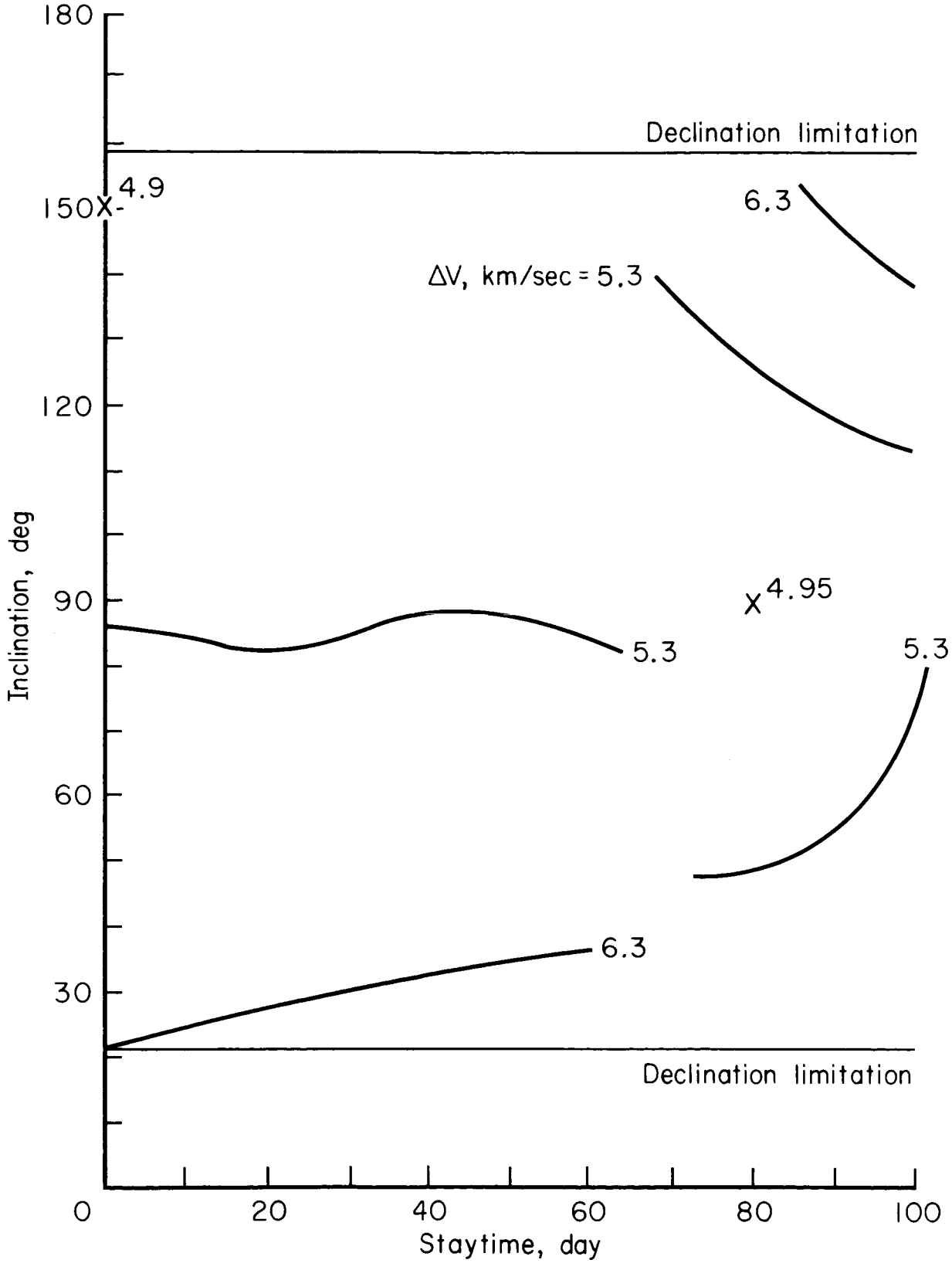

Figure 17(b).

NATIONAL AERONAUTICS AND SPACE ADMINISTRATION
AMES RESEARCH CENTER, MOFFETT FIELD, CALIFORNIA